

**THREE-DIMENSIONAL MODELLING OF EARTH  
RESISTIVITY FOR NON-UNIFORM SOIL CONDITIONS**

K. RAJKUMAR

(159319 E)

Degree of Master of Science in Electrical Engineering

Department of Electrical Engineering

University of Moratuwa

Sri Lanka

March 2020

**THREE-DIMENSIONAL MODELLING OF EARTH  
RESISTIVITY FOR NON-UNIFORM SOIL CONDITIONS**

K. RAJKUMAR

(159319 E)

Dissertation submitted in partial fulfillment of the requirements for the

Degree Master of Science in Electrical Engineering

Department of Electrical Engineering

University of Moratuwa

Sri Lanka

March 2020

## **DECLARATION OF THE CANDIDATE AND SUPERVISOR**

I declare that this is my own work and this dissertation does not incorporate without acknowledgement any material previously submitted for a Degree or Diploma in any other University or institute of higher learning and to the best of my knowledge and belief it does not contain any material previously published or written by another person except where the acknowledgement is made in the text.

Also, I hereby grant to University of Moratuwa the non-exclusive right to reproduce and distribute my dissertation, in whole or in part in print, electronic or other medium. I retain the right to use this content in whole or part in future works (such as articles or books).

.....

Signature of the candidate

(K. Rajkumar)

.....

Date:

The above candidate has carried out research for the Masters Dissertation under my supervision.

.....

Signature of the Supervisor

(Dr. Asanka Rodrigo)

.....

Date:

## **Abstract**

The Grounding Resistance and Soil Resistivity plays a major role for the safe operation of electrical power systems, earthing system design, lightning protection systems etc. the corrosion level underground items like piling pipelines also can be evaluated with ground resistivity profiles.

The researches and standards are mostly referring 2-layer soil conditions and horizontal multi layers, still the results are misinterpreted for different possible types of soil layers.

In this research, three-dimensional modelling of earth resistivity layers done using apparent soil resistivity readings and applying the optimization algorithm. A methodology has been proposed to model the actual soil resistivity and layer thickness for a multi-layered soil structure. The apparent earth resistivity measured using Wenner four - point method. The readings further analyzed with MATLAB using genetic algorithm (GA).

The results provided by the GA Constitute the three-dimensional modelling of actual earth resistivity profile for a non-uniform soil. The nobility of the research is to obtain the multi-layer soil characteristics and conclude it to a three-dimensional model through the measurements in soil electric properties in the top surface soil.

Keywords: Soil Resistivity Measurements, Multilayered Soil, Genetic Algorithms (GSs), Optimization.

## **Acknowledgement**

This research study was carried out in partial fulfillment of the Master of Science in Electrical Engineering at University of Moratuwa.

It is my great pleasure to express gratitude to those who were behind me in completing my research project.

First and foremost, I wish to express my gratitude towards Dr. Asanka Rodrigo for providing this visionary concept to study, the invaluable support and continuous guidance provided throughout the period in order to complete this research.

My sincere thanks go to Mr. Manjula Perera – MD - WindForce (Pvt) Ltd., Prof. W.D. Anura S. Wijayapala - CEO - WindForce (Pvt) Ltd and all my colleagues at WindForce (Pvt) Ltd who helped me in many ways during this period.

Further, I thank to the academic and nonacademic staff of University of Moratuwa, University of Jaffna for the great support they have rendered throughout this research study as well as MSc Program.

Last but not least, I would express my heartiest gratitude and love to my family members who took a lot of burden and patient, which helped me to complete this work in difficult circumstances.

## Table of Contents

<b>DECLARATION OF THE CANDIDATE AND SUPERVISOR .....</b>	<b>i</b>
<b>Abstract.....</b>	<b>ii</b>
<b>Table of Contents .....</b>	<b>iv</b>
<b>List of Figures.....</b>	<b>vi</b>
<b>List of Tables .....</b>	<b>ix</b>
<b>List of Abbreviations.....</b>	<b>ix</b>
<b>1. INRODUCTION .....</b>	<b>1</b>
1.1. <b>Background.....</b>	<b>1</b>
1.2. <b>Objectives of study .....</b>	<b>2</b>
1.3. <b>Motivation.....</b>	<b>2</b>
1.4. <b>Methodology .....</b>	<b>2</b>
<b>2. LITERATURE REVIEW.....</b>	<b>4</b>
<b>3. SOIL LAYER MODELS.....</b>	<b>7</b>
<b>4. CALCULATIONS .....</b>	<b>8</b>
4.1. <b>Soil Model .....</b>	<b>8</b>
4.2. <b>Wenner method .....</b>	<b>13</b>
4.3. <b>Mathematical Model.....</b>	<b>14</b>
4.4. <b>Analysis .....</b>	<b>21</b>
4.4.1. <b>Equation Development .....</b>	<b>21</b>
4.4.2. <b>Genetic Algorithm .....</b>	<b>22</b>
4.4.3. <b>Algorithm Development .....</b>	<b>23</b>
<b>5. FIELD MEASUREMENTS .....</b>	<b>25</b>
5.1. <b>Preliminary Test.....</b>	<b>25</b>

5.2.	<b>Earth Resistivity Measurement Plan</b> .....	27
5.2.1.	<b>Wenner Four Probe Measurement Plan</b> .....	27
5.2.2.	<b>Topsoil Measurement Plan</b> .....	27
5.3.	<b>Location 1</b> .....	28
5.3.1.	<b>Earth Resistivity Wenner Method Measurements</b> .....	29
5.3.2.	<b>Topsoil Resistivity Measurements</b> .....	33
5.4.	<b>Location 2</b> .....	35
5.4.1.	<b>Earth Resistivity Wenner Method Measurements</b> .....	36
5.4.1.	<b>Top Soil Resistivity Measurements</b> .....	39
6.	<b>ANALYTICAL RESULTS</b> .....	41
6.1.	<b>Measurements</b> .....	41
6.2.	<b>Location 1 - 10 MW Solar Power Plant - Vavuniya</b> .....	44
6.2.1.	<b>Results Validation</b> .....	49
6.3.	<b>Location 2 - 20 MW Wind Power Plant - Kilinichchi</b> .....	52
6.3.1.	<b>Results Validation</b> .....	57
7.	<b>CONCLUSIONS AND RECOMMENDATIONS</b> .....	58
7.1.	<b>Achievement of Objective and Research Outcome</b> .....	58
7.2.	<b>Limitations of the study</b> .....	58
7.3.	<b>Applications and Recommendations</b> .....	59
8.	<b>References</b> .....	60

## List of Figures

Figure 3.1: Soil Layers	7
Figure 4.1: Soil Electrical Property Model	8
Figure 4.2: Current Flow in Homogeneous Media due to Single Electrode	9
Figure 4.3: Current Flow in Homogeneous Media due to Two Electrodes	9
Figure 4.4: Current Flow path in 3-Dimensional view and equipotential lines	10
Figure 4.5: Current Flow path variation in soil layers	10
Figure 4.6: Current flow path with different probe spacings	11
Figure 4.7: Apparent Earth Resistivity Graph1	11
Figure 4.8: Apparent Earth Resistivity Graph2	11
Figure 4.9: Wenner method with equally spaced test probes	13
Figure 4.10: Two-layer Earth Model	17
Figure 4.11: Three-layer Earth Model	20
Figure 4.12: Multi-layer Earth Model	20
Figure 4.13: Horizontal Soil Layers	21
Figure 4.14: Global Optimization Approaches	22
Figure 4.15: Data Acquisition of the Algorithm	23
Figure 4.16: Flowchart of GA evaluation process for the proposed framework	24
Figure 5.1: Digital Earth Resistance Meter GEOHM 5	25
Figure 5.2: Apparent Resistivity ( $\rho_a$ ) vs distance between the electrodes	26
Figure 5.3: Apparent Earth Resistivity Reading Measurement Plan	27
Figure 5.4: Soil box for soil resistivity measurement	27
Figure 5.5: Created Soil box for soil resistivity measurement	28
Figure 5.6: Selected area for the field measurement – Location 1	28
Figure 5.7: Selected area on the map	29
Figure 5.8: Earth Resistivity Measurement	29
Figure 5.9: Earth Resistivity Measurement	30
Figure 5.10: Earth Resistivity probe arrangement – Location 1	30
Figure 5.11: Top soil excavation and soil box filling	33
Figure 5.12: Soil box testing for location 1	33



Figure 5.13: Soil box dimensions	34
Figure 5.14: Soil box Readings	34
Figure 5.15: Selected area for the field measurement – Location 2	35
Figure 5.16: Selected area on the map	35
Figure 5.17: Earth Resistivity Measurement	36
Figure 5.18: Earth Resistivity probe arrangement – Location 2	36
Figure 5.19: Top soil excavation and soil box filling	39
Figure 5.20: Soil box testing for location 2	39
Figure 5.21: Soil box dimensions	40
Figure 5.22: Soil box Readings	40
Figure 6.1: Wenner four probe earth resistivity measurement method	41
Figure 6.2: 1 m Probe Spacing Data Coordinates	41
Figure 6.3: 2 m Probe Spacing Data Coordinates	42
Figure 6.4: 3 m Probe Spacing Data Coordinates	42
Figure 6.5: 4 m Probe Spacing Data Coordinates	43
Figure 6.6: 5 m Probe Spacing Data Coordinates	43
Figure 6.7: 1 m Probe Spacing Resistivity Data Plot	44
Figure 6.8: 2 m Probe Spacing Resistivity Data Plot	44
Figure 6.9: 3 m Probe Spacing Resistivity Data Plot	45
Figure 6.10: 4 m Probe Spacing Resistivity Data Plot	45
Figure 6.11: 5 m Probe Spacing Resistivity Data Plot	46
Figure 6.12: All Probe Spacing Resistivity Readings Data Plot – Location 1	46
Figure 6.13: Final Results- 3 D Modelling of Earth Resistivity for Location 1	49
Figure 6.14: Borehole Locations	49
Figure 6.15: Borehole excavation	50
Figure 6.16: Borehole Location 1	50
Figure 6.17: Rock at 2m Depth	50
Figure 6.18: Rock Sample from the Large Bed Rock	50
Figure 6.19: Borehole Location 2	51
Figure 6.20: Borehole up to 3.5 m	51
Figure 6.21: 1 m Probe Spacing Resistivity Data Plot	52
Figure 6.22: 2 m Probe Spacing Resistivity Data Plot	52

Figure 6.23: 3 m Probe Spacing Resistivity Data Plot	53
Figure 6.24: 4 m Probe Spacing Resistivity Data Plot	53
Figure 6.25: 5 m Probe Spacing Resistivity Data Plot	54
Figure 6.26: All Probe Spacing Resistivity Readings Data Plot – Location 2	54
Figure 6.27: Final Results- 3 D Modelling of Earth Resistivity for Location 2	57

## List of Tables

Table 4.1: Average soil resistivity for common soil types	12
Table 5.1: Resistivity Measurements	26
Table 5.2: Apparent Earth Resistivity Readings – Location 1	31
Table 5.3: Soil box Measurements	34
Table 5.4: Apparent Earth Resistivity Readings – Location 2	37
Table 5.5: Soil box Measurements	40
Table 6.1: Apparent Resistivity Readings from the Data Plot	47
Table 6.2: Final Results from the Genetic Algorithm Optimization	48
Table 6.3: Apparent Resistivity Readings from the Data Plot	55
Table 6.4: Final Results Generated with Genetic Algorithm Optimization	56

## List of Abbreviations

Abbreviation	Description
IEEE	Institute of Electrical and Electronics Engineers
BS	British Standards
GA	Genetic Algorithm

## List of Appendices

Appendix	Description
Appendix A	Soil test report of 20 MW Wind Power Plant, Kilinochchi
Appendix B	Research Papers

### 1. INRODUCTION

#### 1.1. Background

The Grounding Resistance and Soil Resistivity plays a major role in designing and the safe operation of electrical power systems, earthing system design, lightning protection systems etc. The best grounding system and lightning protection system prevents the extreme ground fault and ground potential rise. Grounding system for power stations, facility, sub stations, and general system protection could be able to handle the anticipated fault current. The adequate number of earth mats, rods and other alternatives must be sized in terms of number of earth rods and dimensions to achieve the low earth resistance. The resistivity profile of the soil derived from appropriate soil modelling should be supported to optimize the earthing system design. Determination of ground resistivity profiles will be used to define the corrosion level of underground utilities like piling, pipelines.

The parameters of the earth structure are mandated for the field simulations of grounding systems. There are various models and methodologies available to measure the soil resistivity. Most of them are uniform, two layered and horizontal multilayered soil models.

All these soil models are based on horizontal layers. But in real scenario the soil layers vary three dimensionally. So, the existing models are misinterpreted with the uneven layer patterns. There are few examples for the non-uniform soil conditions like filled land with different types of soil, manmade boundary walls with a large amount of soil filling, slope lands, high boulder areas, etc.

Identification of soil layers and three-dimensional modelling of earth resistivity are most important to minimize the errors and optimize the grounding system in design stage.

## 1.2. Objectives of study

Three-dimensional modelling of earth resistivity with the help of apparent earth resistivity readings.

## 1.3. Motivation

This study helps to get the exposure of three-dimensional modelling the soil layers with the help of apparent soil resistivity readings. This will be useful to the grounding system designers to design a more accurate system with minimum error which improves the reliability and safety of an electrical installation.

## 1.4. Methodology

The main steps of this research are listed below

1. Understand the different soil layer models with both vertical and horizontal soil layer compositions.

The purpose of this research is to explain the more complex structures rather than just horizontal and vertical layer soil. The source data acquired from an array of points per locations and interpolated separately for each probe spacing. This interpolated data used as a source data for the three-dimensional model.

2. Derive the equation/model to calculate the soil resistivity with the help of apparent soil resistivity readings.

There is already an equation available for two-layer soil model. IEEE standard recommends Sunde Equation for the two-layer soil. [1] This equation is extended to horizontal multilayer soil model and derived a new equation.

3. Earth resistivity data collected to obtaining multilayer electrical properties with Wenner four-probe method.  
BS and IEEE Standards refers the Wenner four-probe method as a best method to measure the apparent earth resistivity. [2] So, this method is used to get the array of earth resistivity readings
4. Simulations for multilayer earth structures conducted with Genetic Algorithm using MATLAB 2009 including boundary element formulation. Estimate soil resistivity  $\rho$ , thickness  $t$  with four probe soil resistivity measurements.  
GA is the best optimization tool to find the global minimum when there are multiple local minimums available. [3] The Sunde's equation is modified to apply the GA and found the optimum combinations of layer height and resistivities of each point
5. Three-dimensional modelling of earth resistivity derived from the Wenner method based on apparent earth resistivity readings and topsoil earth resistivity readings.  
Measure the topsoil reading separately and combine all the readings. Draw the three-dimensional soil resistivity profile.
6. Validate the results.

## CHAPTER 2

### 2. LITERATURE REVIEW

The international standards are referring the uniform, horizontal two layer and horizontal multi-layer soil conditions in earth resistivity, electrical installation earthing and ground system designs. But in real situation the soil profile has to express in three-dimensional model which is not uniform. The soil is a combination of horizontal and vertical layers.

This literature review is analyzing the British Standards, IEEE standards and some other research papers to identify the research gap and define the proper method to find the soil layers for the three-dimensional modelling.

1. BS 7430:2011 Code of practice for protective earthing of electrical installations [2]
  - Wenner Four-Point method is suggested as a good method to measure Apparent Resistivity.
  - It does not mention any thing about soil layers.
  - Formulae are all based on homogeneous soil.
  - Formulae often give results within 15% accuracy

Standard states “The resistance to earth of a given electrode depends upon the electrical resistivity of the soil. Most first approximation formulae are related to homogenous soil, which is rarely the case in practice, where the different layers of strata will affect the distribution of current passing through the electrode.”

2. IEEE Guide for Measuring Earth Resistivity, Ground Impedance, and Earth Surface Potentials of a Grounding System IEEE Std 81™-2012 (Revision of IEEE Std 81-1983) [1]
  - Prefers Wenner Four-Point method as a good method to measure Apparent Resistivity.
  - Standard discusses Homogeneous and Horizontal two layered Soil



- It does not include Multi-layered Horizontal or Vertical layered Soil (Three-Dimensional Modelling)
3. Analysis of Earth Resistance of Electrodes and Soil Resistivity at Different Environments [4]
- Author(s): Lee Weng Choun, Mohd Zainal, Chandima Gomes, Wan Fatinhamamah  
2012 International Conference on Lightning Protection (ICLP), Vienna, Austria
- This paper analyzes the results about several site earth measurements, measurement deviations and pattern.
  - Paper Briefs about following aspects.
    - The Soil Resistivity vary Considerably (more than 50%) within a few meters distance for a specific Site.
    - Soil Resistivity decreases once it moves towards vegetation
    - Near water and Near Built-up area, soil structure may be loosely bound. So, it shows a low resistivity value.
4. Estimation of Soil Electrical Properties in a Multilayer Earth Model with Boundary Element Formulation [5]
- Author(s): T. Islam, Z. Chik, M.M. Mustafa and H. Sanusi  
Mathematical Problems in Engineering Volume 2012, Hindawi Publishing Corporation
- This paper presents an effective model for estimation of soil electric resistivity with depth and layer thickness in a multilayer earth structure.
  - The theoretical equation with numerical analysis on soil electric field are derived for Horizontally Multilayer soil investigations.
5. Study of Soil Resistivity Measurements in Vertical Two-Layer Soil Model. [6]
- Author(s): Mohamed Nayel, Boyang Lu, Yu Tian, Yingzhen Zhao  
Xi'an Jiaotong-Liverpool University Suzhou, China.
- This paper studies and estimates soil resistivity parameters of two-layer vertical soil model

- Gauss-Newton method is used to estimate the soil parameters with the equation
  - The apparent measured resistivity in vertical layer soil derived
6. A Simple formula of Grounding Grid Resistance in Vertical Two-Layer Soil. [7]  
 Author(s): Xiaobin Cao, Guangning Wu, Shenglin Li, Weiming Zhou and RuiFang.Li
- This paper analyzes the error range of CDEGS software simulation vs real value for grounding grid in vertical double layer soil under different conditions.
  - The equation is not verified with practical data and this equation can be applied only for the grounding grids.
  - The Grid Buried in Uniform Medium has a fixed relationship with grounding resistance.
7. Analysis of Linear Ground Electrodes Placed in vertical Three-Layer Earth. [8]  
 Author(s): Predrag D. Rancid, Zoran P. Stajic, Bojana S. ToSic  
 IEEE TRANSACTIONS ON MAGNETICS. VOL 12, NO 3, MAY 1996
- Three Vertical Layers of Soil has been analyzed in this research.
  - The complex conductivity enabled implementation of the mathematical model and calculation of the LGE equivalent capacitance were analyzed.
  - Magnetic field distribution around the LGE is also successfully determined by using the Ampere-Laplace formula.

3. SOIL LAYER MODELS

Soil is having a complex structure with the combination of several materials and compositions. Most of the time the soil can be modeled with horizontal layers or vertical layers or combination of both in different shapes. These parameters are important for the simulation of earthing and other designs.

By considering a unit area in the soil, the soil layers can be reduced to horizontal layers. Sunde’s equation for horizontal two-layer model can be used to derive the equation for horizontal multilayer soil model. This horizontal multilayer soil resistivity equation can be used to find the soil layer thickness and soil layer average resistivity for each unit area with the help of boundary conditions and optimization technique.

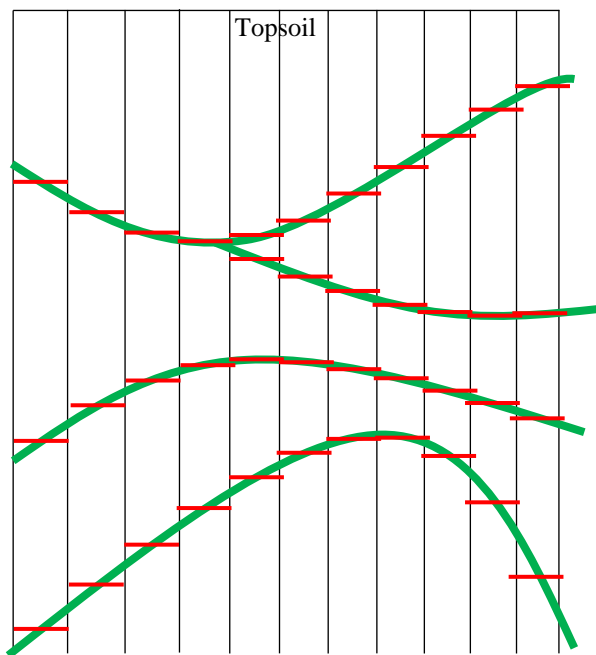


Figure 3.1: Soil Layers

Consider a soil layer variation shown in Figure 3.1. The different 3 D variations in the soil can be divided into several unit areas and reduced to a horizontal layer soil model. Then it is possible to apply the horizontal multi-layer soil model equation and get the individual results using optimization technique separately and draw the three-dimensional Soil Model.

## CHAPTER 4

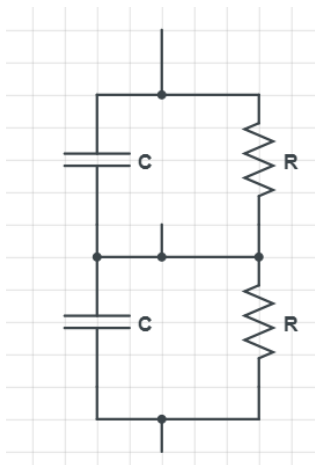
### 4. CALCULATIONS

“Sunde Equation” is used for accurate and equivalent mathematical modelling of multi layered soil. Wenner four-point method is used to measure the apparent resistivity. three-dimensional modelling of earth resistivity is done based on the mathematical model developed and the apparent resistivity readings.

#### 4.1. Soil Model

Current Flow in Soil can be categorized as following [9]

- Electrolytic Conduction
  - Occurs by relatively slow migration of ions in a fluid electrolyte
  - Controlled by type of ion, ion concentration and ionic mobility
- Electronic Conduction
  - Occurs in metals by rapid movement of electrons
  - Found in native metals and some metal oxides and sulphide ores
- Dielectric Conduction
  - Occurs in weakly conducting materials, or insulators, in presence of external alternating current
  - Atomic electrons are shifted slightly relative to nucleus



Soil Behave as a Lossy media can be modeled as

- A Conductor with Resistance R
- A Dielectric

Except for high frequency and step front wave penetration, Charging Current is negligible compared to Leakage Current. [10]

Figure 4.1: Soil Electrical Property Model

Also, this research is using Wenner four probe method to measure the apparent earth resistivity, which is using direct current for the measurement of apparent resistivity.

So, Earth can be represented by a pure resistance.

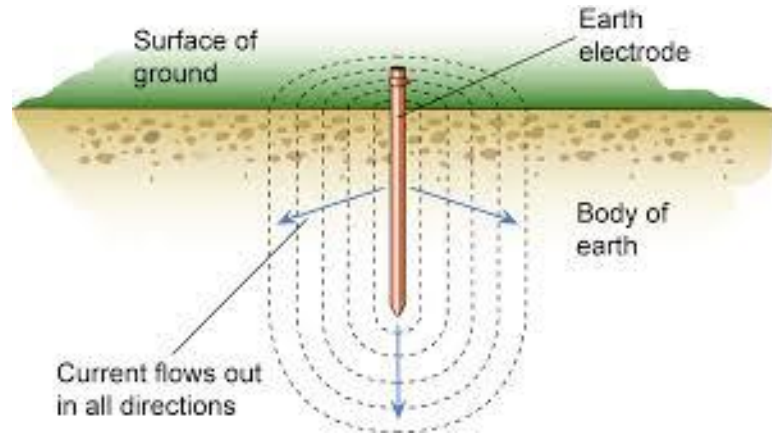


Figure 4.2: Current Flow in Homogeneous Media due to Single Electrode

Current spread out Vertically and Horizontally (Radially)

Potential at any point at the surface of Half-Space is  $V = \frac{\rho I}{2\pi r}$  (4.01)

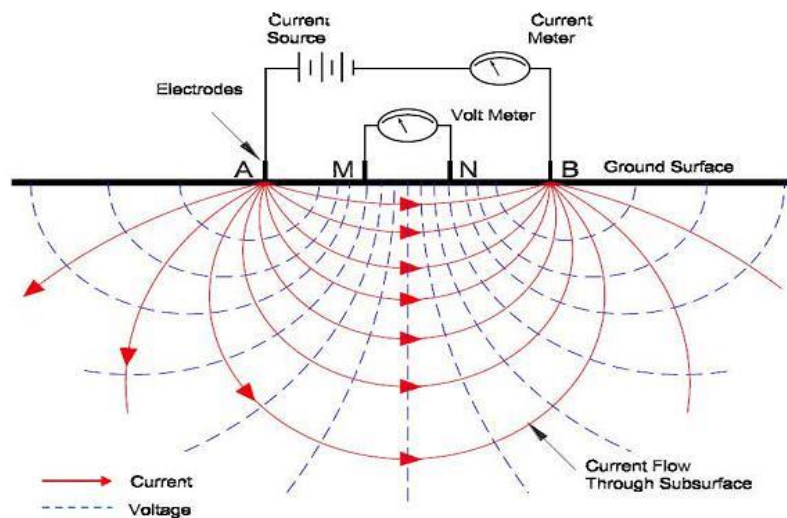


Figure 4.3: Current Flow in Homogeneous Media due to Two Electrodes

Source: Application of Vertical Electrical Sounding [11]

This research presents the optimum method to estimate the earth resistivity of each soil layer and the layer thicknesses of a multilayer soil structure. This mathematical model is the improvement of two-layer conventional earth model with boundary conditions.

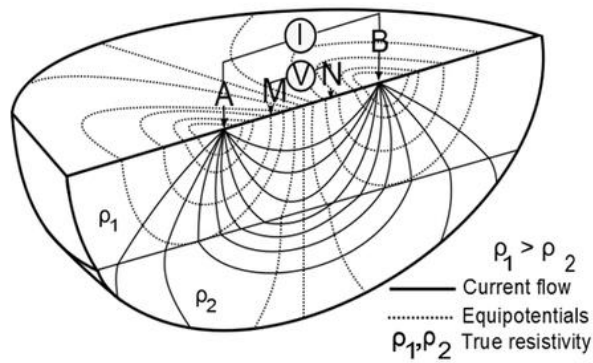


Figure 4.4: Current Flow path in 3-Dimensional view and equipotential lines

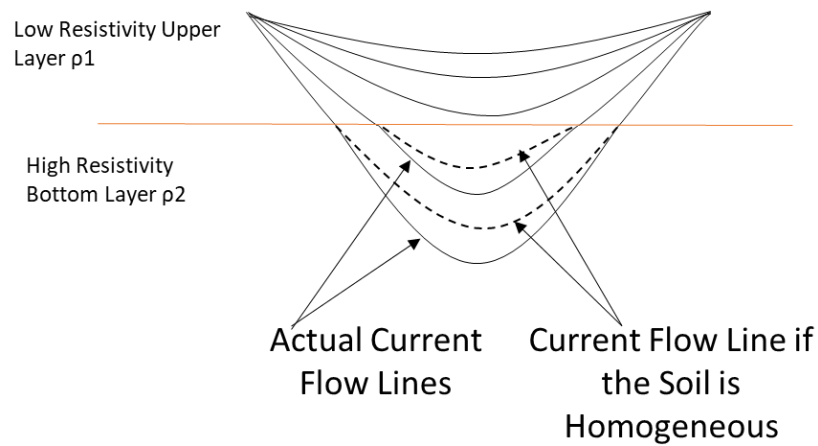


Figure 4.5: Current Flow path variation in soil layers

Most of the soils with various soil layers in three dimensional variations, the multi-layer soil resistivity model is more suitable to identify the soil resistivity variations like soil types, anomalous materials in soil, density of compacted soil etc.

The apparent resistivity measurements taken by changing the probe spacing will give different values with considerable variations according to the number of soil layers

directly inside the soil. According to Figure 4.6, when the probe distance increases, the current penetration into soil increases to higher depths.

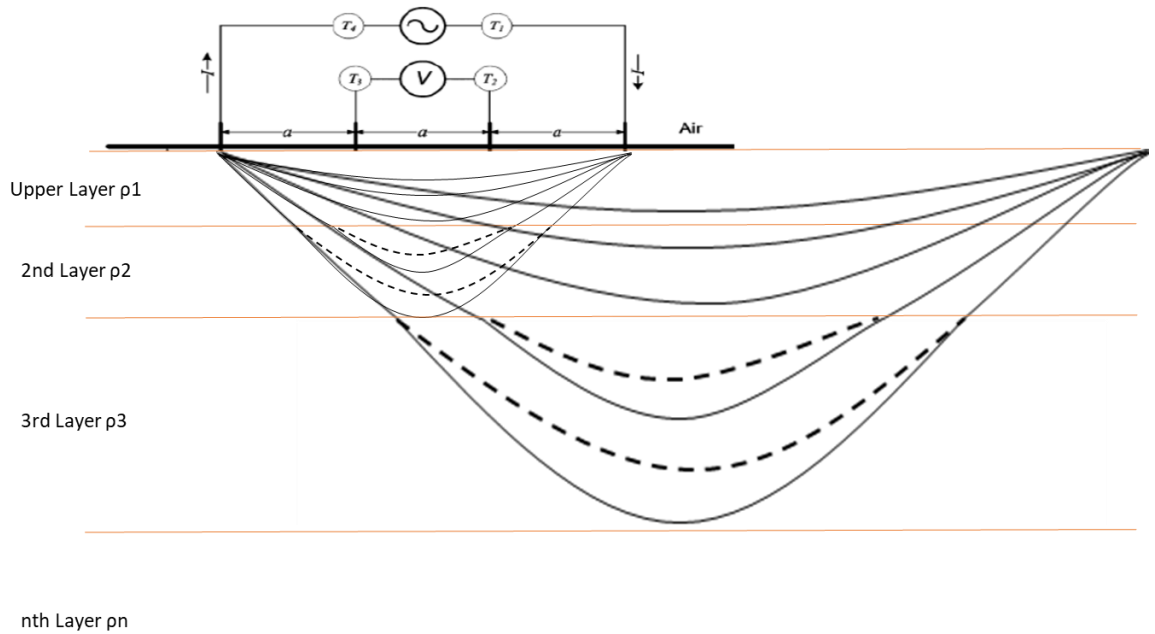


Figure 4.6: Current flow path with different probe spacings.

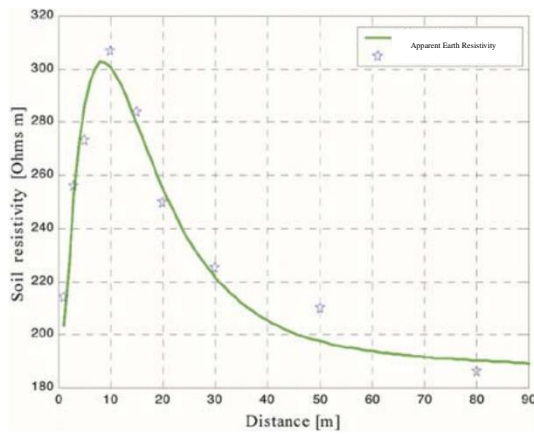


Figure 4.7: Apparent Earth Resistivity Graph1

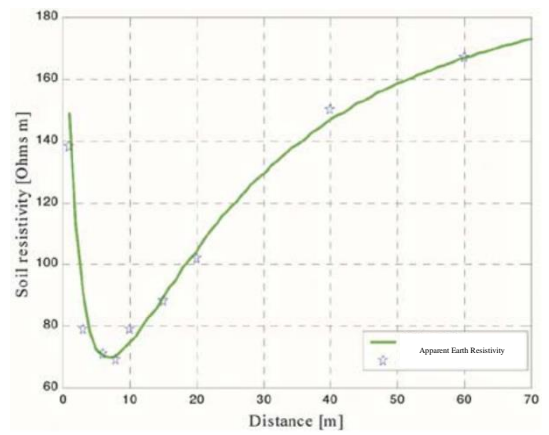


Figure 4.8: Apparent Earth Resistivity Graph2

Source: IEEE transactions on power delivery Research Paper [3]

Figure 4.7 and Figure 4.8 shows three-layer soil model earth resistivity readings varying with the probe spacing.

In Figure 4.7, the earth resistivity increases at the beginning and decreases drastically for the higher probe spacings. It can be concluded that the middle soil layer is having a higher soil resistivity. [3]

In Figure 4.8, the earth resistivity decreases at the beginning and increasing drastically for the higher probe spacings. It can be concluded that the middle soil layer is having a lower soil resistivity. [3]

Different soil compositions having various soil resistivities. Table 4.1 shows the average soil resistivity ranges for the known soil materials. It is possible to predict the soil type by knowing the actual earth resistivities of each soil layers

Table 4.1: Average soil resistivity for common soil types

	<b>Soil</b>	<b>Average Resistivity (<math>\Omega</math> m)</b>
1	Clay, compacted	100 - 200
2	Clay, soft	50
3	Clayey sand	50 - 500
4	Humus, leaf mould	10 - 150
5	Granite	1500 - 10000
6	Granite, modified	100 - 600
7	Jurassic marl	30 - 40
8	Limestone, fissured	500 - 1000
9	Marl	100 - 200
10	Mica schist	800
11	Peat, turf	5 - 100
12	Sandstone	1500 - 10000
13	Sandstone, modified	100 - 600
14	Schist, shale	50 - 300
15	Siliceous sand	200 - 300
16	Soil, chalky	100 - 300
17	Soil, swampy	1 - 30
18	Stony sub-soil, grass covered	300 - 500
19	Stony ground	1500 - 3000

Source: Monte Carlo Simulation Approach to Soil Layer Resistivity Modelling for Grounding System Design [12]



#### 4.2. Wenner method

BS and IEEE standards are referring the Wenner four probe method as the best method to measure the Earth apparent resistivity of undistributed earth. [1] It is developed by Dr. Frank Wenner, US Bureau of Standards in 1915.

There are Four number of probes use for this measurement. The outer electrodes which injects current to the earth called current electrodes. The current passing through the outer electrodes creates a voltage difference of the inner electrodes because of the earth resistance. This is called fall of potential method. Both Current and Voltage drop are measured and used to calculate the apparent resistivity of the earth.

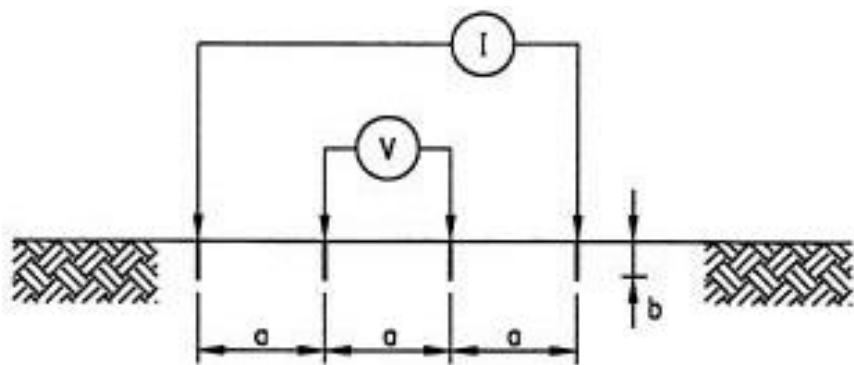


Figure 4.9: Wenner method with equally spaced test probes

A current  $I$  is passed between the outer probes, and at the same time potential  $V$  between the inner probes is measured using a potentiometer or high-impedance voltmeter. Then, the apparent resistivity  $\rho$  can be defined in the terms of length  $a$  and  $b$ .

$$\rho = \frac{4\pi a R}{1 + \frac{2a}{\sqrt{a^2 + 4b^2}} - \frac{a}{\sqrt{a^2 + b^2}}} \quad (4.02)$$

$\rho$  = Resistivity

$b$  = Depth of Probes

$a$  = Spacing of Probes

$R$  = Resistance (reading from meter)

in practice, the electrodes are usually placed in a straight line at intervals  $a$ , driven to a depth not exceeding  $0.1a$ . Then, we can assume  $b = 0$  and the equation becomes

$$\rho = 2\pi a R$$

$$\rho = 2\pi a \frac{V}{I} \quad (4.03)$$

#### 4.3. Mathematical Model

For the particular case of a stationary current entering a uniform or horizontally stratified earth, over a spherical electrode or a cylindrical electrode perpendicular to the surface of the earth, the formula solution for continuous variation in resistivity with depth can be derived from the basic equation. The equation and their solution are presented here [13].

Assume that the earth conductivity  $\sigma = \sigma(x,y,z)$  can be expressed as a function of the point coordinates and the earth imagined as isotropic, then the conductivity of the earth in all direction are same.

So, the following equations can be written about the current density

$$J_x = \sigma E_x \quad J_y = \sigma E_y \quad J_z = \sigma E_z \quad (4.04)$$

If the earth potential at any arbitrary point is  $U$ , along the three axis the electrical intensities can be written as

$$E_x = -dU/dx \quad E_y = -dU/dy \quad E_z = -dU/dz \quad (4.05)$$

Another basic equation of current density,  $J$  is that

$$\text{div } J = 0$$

$$\frac{dJ_x}{dx} + \frac{dJ_y}{dy} + \frac{dJ_z}{dz} = 0 \quad (4.06)$$

With (4.04) and (4.05) in (4.06), the following equation can be obtained:

$$\frac{d^2U}{dx^2} + \frac{d^2U}{dy^2} + \frac{d^2U}{dz^2} + \frac{1}{\sigma} \left[ \frac{dU}{dx} \frac{d\sigma}{dx} + \frac{dU}{dy} \frac{d\sigma}{dy} + \frac{dU}{dz} \frac{d\sigma}{dz} \right] = 0 \quad (4.07)$$

Assume the conductivity  $\sigma$  is varying only with depth  $z$ . Then conductivity will be a function of  $z$ . So,  $\sigma = \sigma(z)$  and can say  $d\sigma/dx$  and  $d\sigma/dy = 0$ .

Then the electric field will be symmetrical along the  $z$  axis. So, cylindrical coordinates can be introduced ( $r = \sqrt{x^2 + y^2}$ ) and obtained the following equation:

$$\frac{d^2U}{dr^2} + \frac{1}{r} \frac{dU}{dr} + \frac{d^2U}{dz^2} + \frac{dU}{dz} \frac{\sigma'(z)}{\sigma(z)} = 0 \quad (4.08)$$

Where  $\sigma'(z) = d\sigma(z)/dz$ .

Due to the azimuthal symmetry, we can separate (4.08) using separation of variables as  $U(r,z) = u(r) v(z)$ , which is a product of a function of  $r$  and a function of  $z$ . Thus,

$$\frac{d^2u}{dr^2} + \frac{1}{r} \frac{du}{dr} + \lambda^2 u = 0 \quad (4.09)$$

Where  $u$  is the vector of cylindrical coordinates.

And

$$\frac{d^2v}{dz^2} + \frac{\sigma'(z)}{\sigma(z)} \frac{dv}{dz} - \lambda^2 v = 0 \quad (4.10)$$

Where  $\lambda$  is an arbitrary constant.

Equation (4.09) is the zero order Bessel function. The equation (4.10) can be identified as a plane wave propagation and the conductivity of the medium changes along the wave propagation direction. The conductivities of longitudinal and transverse direction also change in the same manner. So, the propagation constant  $\lambda$  remains unchanged.

So, the electric potential can be expressed in general as

$$U = \int_0^\infty g(\lambda) u(\lambda, r) v(\lambda, z) d\lambda \quad (4.11)$$

Where  $g(\lambda)$  is a function of  $\lambda$  only, to satisfy certain boundary conditions.

Equation (4.09) is satisfied by the Bessel function of the first and second kind,  $J_0(\lambda r)$  and  $Y_0(\lambda r)$ . Since the potential remains finite for  $r = 0$  (except if  $z = 0$  at the same time), while the function  $Y_0$  has a singularity at  $r = 0$ .

By applying a boundary condition at the earth surface, the electric force must vanish in the  $z$  direction. So, current is zero in the  $z$  direction. Hence, for  $z = 0$ ,

$$\frac{dU}{dz} = \int_0^{\infty} g(\lambda) J_0(\lambda r) v'(\lambda, z) d\lambda = 0 \quad (4.12)$$

Where  $v'(\lambda, z) = dv/dz$

Equation (4.12) is satisfied by  $g(\lambda) = A \lambda/v'(\lambda, 0)$  where  $A$  is a constant, since the integral vanishes when the integrand equals  $\lambda J_0(\lambda r) d\lambda$ . Hence

$$U = A \int_0^{\infty} J_0(\lambda r) k(\lambda, z) d\lambda$$

$$k(\lambda, z) = \frac{\lambda v(\lambda, z)}{v'(\lambda, 0)}$$

Equation (4.10) having a pair of solutions  $e^{\pm\lambda z}$  for a uniform earth. Since the potential vanishes at infinity, the negative sign is considered. Therefore, for a uniform earth,

$$U = A \int_0^{\infty} J_0(\lambda r) e^{-\lambda z} d\lambda = A \sqrt{(r^2 + z^2)}$$

The potential at a uniform earth solution can be obtained as

$$U = (I\rho/2\pi) \sqrt{(r^2 + z^2)}, \text{ So, } A \text{ can be expressed by } A = I\rho/2\pi,$$

Where,  $\rho$  is the earth resistivity and  $I$  is the current in the electrode.

With the variation of the depth, the resistivity also varies arbitrarily, the ratio of potential at a point on the surface of the earth to current entering electrode can be expressed as the mutual resistance of the electrode can be written as,

$$\rho = \frac{\rho_0}{2\pi} \int_0^{\infty} k(\lambda) J_0(\lambda r) d\lambda$$

Where  $\rho_0 = \rho(0)$  is the resistivity at the surface and  $k(\lambda) = k(\lambda, 0)$

## Two-Layer Equation

Assume that earth surface layer is having a depth of  $h_1$  and average earth resistivity of  $\rho_1$  and lower layer having an infinity depth and average earth resistivity of  $\rho_2$ .

It is assumed that the resultant field having two components since the conventional method to solve these similar problems are assumed to have two components. One is primary and other one is secondary. Primary is by the electric field in uniform soil condition. The secondary component is due to the charges or current induced due to the primary electric field. The resultant upper- and lower-layer potentials  $U_1$ ,  $U_2$  can be written thus

$$U_1 = U' + U_1''$$

$$U_2 = U' + U_2''$$

The primary field is  $U'$ , the upper layer secondary field is  $U_1''$  and the lower layer secondary field is  $U_2''$ .

When considering a single electrode, and the  $z$  axis is going into the earth, there is a circular symmetry around the  $z$  axis. So, the potential at any point is depend on the radial distance  $r$  and  $z$ .  $r$  is the distance from the electrode parallel to earth surface.

For the upper layer with a uniform soil resistivity

$$U' = \frac{I\rho_1}{2\pi} \sqrt{(r^2 + z^2)}$$

The  $\sqrt{(r^2 + z^2)}$  can be express using the Fourier transformation as below

$$\sqrt{(r^2 + z^2)} = \int_0^\infty f(\lambda r) e^{-\lambda z} d\lambda$$

Where

$$f(\lambda r) = \frac{1}{2\pi i} \int_{-i\infty}^{i\infty} e^{\lambda z} \sqrt{(r^2 + z^2)} dz = J_0(\lambda r)$$

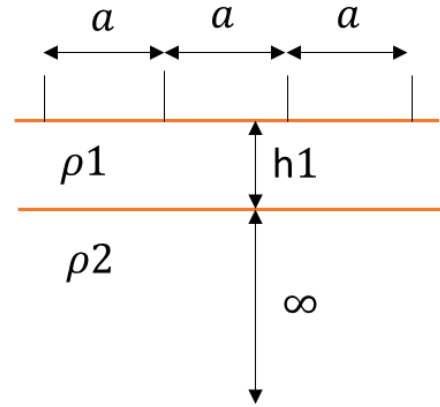


Figure 4.10: Two-layer Earth Model

$$\text{So, } U' = \frac{i\rho_1}{2\pi} \int_0^\infty e^{-\lambda z} J_0(\lambda r) d\lambda$$

Same as this, the secondary potentials can be written by multiplying with an arbitrary function of  $\lambda$

$$U_1'' = \int_0^\infty [f_1(\lambda)e^{-\lambda z} + g_1(\lambda)e^{\lambda z}] J_0(\lambda r) d\lambda$$

$$U_2'' = \int_0^\infty [f_2(\lambda)e^{-\lambda z} + g_2(\lambda)e^{\lambda z}] J_0(\lambda r) d\lambda$$

Applying the boundary conditions

At the surface of the earth

$$E_z = -dU/dz = 0$$

$$\text{So, } f_1 = g_1$$

When  $z = \text{infinity}$ , the potential vanishes.

$$\text{So, } g_2 = 0$$

When the boundary condition  $z = h_1$ , functions  $f_1$  and  $f_2$

The potentials  $U_1$  and  $U_2$  must be equal. Also, the current densities  $J_1, J_2$  in  $z$  direction need to be equal.

$$J_1 = -(1/\rho_1) dU_1/dz$$

$$J_2 = -(1/\rho_2) dU_2/dz$$

From the above boundary condition, the following equations can be obtained

$$U_1 = U_2$$

$$U' + U_1'' = U' + U_2''$$

$$U_1'' = U_2''$$

$$\int_0^\infty [f_1(\lambda)e^{-\lambda h_1} + f_1(\lambda)e^{\lambda h_1}] J_0(\lambda r) d\lambda = \int_0^\infty [f_2(\lambda)e^{-\lambda h_1}] J_0(\lambda r) d\lambda$$

$$f_1(\lambda)e^{-\lambda h_1} + f_1(\lambda)e^{\lambda h_1} = f_2(\lambda)e^{-\lambda h_1}$$

$$J1 = J2$$

$$-(1/\rho_1) dU1/dz = -(1/\rho_2) dU2/dz$$

$$\begin{aligned} \frac{1}{\rho_1} \left[ \frac{I\rho_1}{2\pi} \int_0^\infty e^{-\lambda h_1} J_0(\lambda r) d\lambda + \int_0^\infty [f_1(\lambda)e^{-\lambda h_1} + f_1(\lambda)e^{\lambda h_1}] J_0(\lambda r) d\lambda \right] \\ = \frac{1}{\rho_2} \left[ \frac{I\rho_1}{2\pi} \int_0^\infty e^{-\lambda h_1} J_0(\lambda r) d\lambda + \int_0^\infty [f_2(\lambda)e^{-\lambda h_1}] J_0(\lambda r) d\lambda \right] \end{aligned}$$

$$\frac{\lambda}{\rho_1} \left[ \frac{I\rho_1}{2\pi} e^{-\lambda h_1} + f_1(\lambda)(e^{-\lambda h_1} + e^{\lambda h_1}) \right] = \frac{\lambda}{\rho_2} \left[ \frac{I\rho_1}{2\pi} e^{-\lambda h_1} + f_2(\lambda)e^{-\lambda h_1} \right]$$

Solution of those equations

$$f_1(\lambda) = \frac{I\rho_1}{2\pi} \frac{-\mu_1 e^{-2\lambda h_1}}{1 + \mu_1 e^{-2\lambda h_1}}$$

$$\text{Where } \mu_1 = \frac{\rho_1 - \rho_2}{\rho_1 + \rho_2}$$

$$\rho_c(r) = \int_0^\infty \left[ \frac{\rho_1}{2\pi} + 2f_1(\lambda) \right] J_0(\lambda r) d\lambda$$

$$\rho_c(r) = \frac{\rho_1}{2\pi} \int_0^\infty \left[ \frac{1 - \mu_1 e^{-2\lambda h_1}}{1 + \mu_1 e^{-2\lambda h_1}} \right] J_0(\lambda r) d\lambda$$

$$\rho_c(a) = \frac{\rho_1}{2\pi} \int_0^\infty k_{12}(\lambda) J_0(\lambda a) d\lambda$$

Where

$$k_{12}(\lambda) = \frac{1 - \mu_{12}(\lambda)e^{-2\lambda h_1}}{1 + \mu_{12}(\lambda)e^{-2\lambda h_1}}$$

$$\mu_{12}(\lambda) = \frac{\rho_1 - \rho_2}{\rho_1 + \rho_2}$$

$\rho_c$ - Calculated Apparent Resistivity

$\lambda$  – Integration Variable

$a$ - Distance between Electrodes

### Three Layer Equation

$$\rho_c(r) = \frac{\rho_1}{2\pi} \int_0^\infty \left[ \frac{1 - \mu_{12}(\lambda)e^{-2\lambda h_1}}{1 + \mu_{12}(\lambda)e^{-2\lambda h_1}} \right] J_0(\lambda r) d\lambda$$

$$\mu_{12}(\lambda) = \frac{\rho_1 - \rho_2 \left[ \frac{1 - \mu_{23}(\lambda)e^{-2\lambda h_2}}{1 + \mu_{23}(\lambda)e^{-2\lambda h_2}} \right]}{\rho_1 + \rho_2 \left[ \frac{1 - \mu_{23}(\lambda)e^{-2\lambda h_2}}{1 + \mu_{23}(\lambda)e^{-2\lambda h_2}} \right]}$$

$$\mu_{23}(\lambda) = \frac{\rho_2 - \rho_3}{\rho_2 + \rho_3}$$

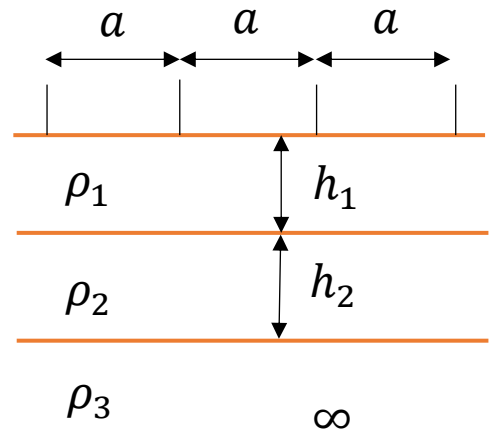


Figure 4.11: Three-layer Earth Model

### Multi-Layer Equation

$$\rho_c(a) = \frac{\rho_1}{2\pi} \int_0^\infty k_{12\dots n}(\lambda) J_0(\lambda a) d\lambda$$

$$k_{12\dots n}(\lambda) = \frac{1 - \mu_{12\dots n}(\lambda)e^{-2\lambda h_1}}{1 + \mu_{12\dots n}(\lambda)e^{-2\lambda h_1}}$$

$$\mu_{12\dots n}(\lambda) = \frac{\rho_1 - \rho_2 k_{12\dots n}}{\rho_1 + \rho_2 k_{12\dots n}}$$

$\rho_c$ - Calculated Apparent Resistivity

$\lambda$  – Integration Variable

$a$ - Distance between Electrodes

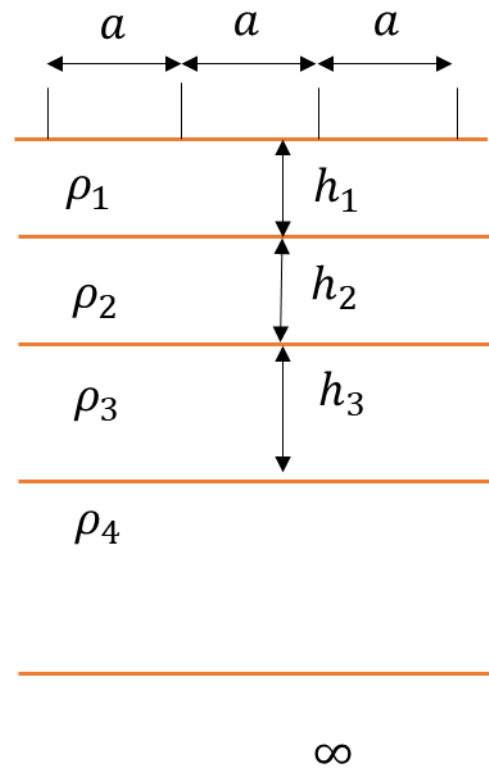


Figure 4.12: Multi-layer Earth Model

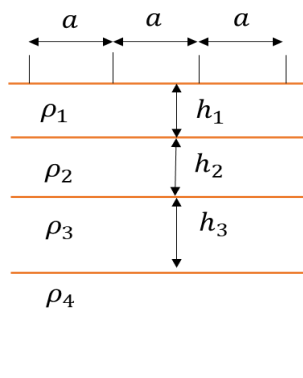


#### 4.4. Analysis

##### 4.4.1. Equation Development

Actual apparent resistivity is available with the measured data. The mathematical model is developed to calculate the number of layers, layer thickness and the average resistivity of those layers with the help of apparent resistivity for a multi-layer soil model. These measured apparent resistivity readings have to use as an input for the derived equation for the multi-layer soil structure. It is needed to find the layer thickness and layer average resistivities.

Since there are multiple variables involve in this mathematical problem, this need to be adjusted as an optimization problem by applying boundary conditions. So, the multilayer soil resistivity equation is transformed as a minimization problem to apply the optimization approach.



$$F \text{ error} = \sum_{n=1}^N \left| \frac{\rho_m - \rho_c}{\rho_c} \right|$$

N – Total Number of Measured Apparent Resistivity

$\rho_m$  - Measured Apparent Resistivity

$\rho_c$ - Calculated Apparent Resistivity

Figure 4.13:  $\infty$  Horizontal Soil Layers

Total number of readings taken per location in this research by changing the probe spacing is five (1 m to 5 m). In an ideal condition, if the number of layers, layer thickness and layer average resistivities are known values,  $\rho_m$  and  $\rho_c$  have to be equal and F(error) should be zero. But in practical it is difficult to identify the values without error. In the single objective optimization problems, there is a single optimal solution. But in multi objective optimization problems having a set of different optimum solutions. [14] It is required to find the most suitable values from the set of optimum solutions. So, this research can be concluded with the nearby values of layer thickness and layer average resistivity by finding the Global Minimum of F(error).

#### 4.4.2. Genetic Algorithm

There are several techniques available for the optimization problems. Within that Evolutionary Computation is the most efficient technique to find the Global Minimums.

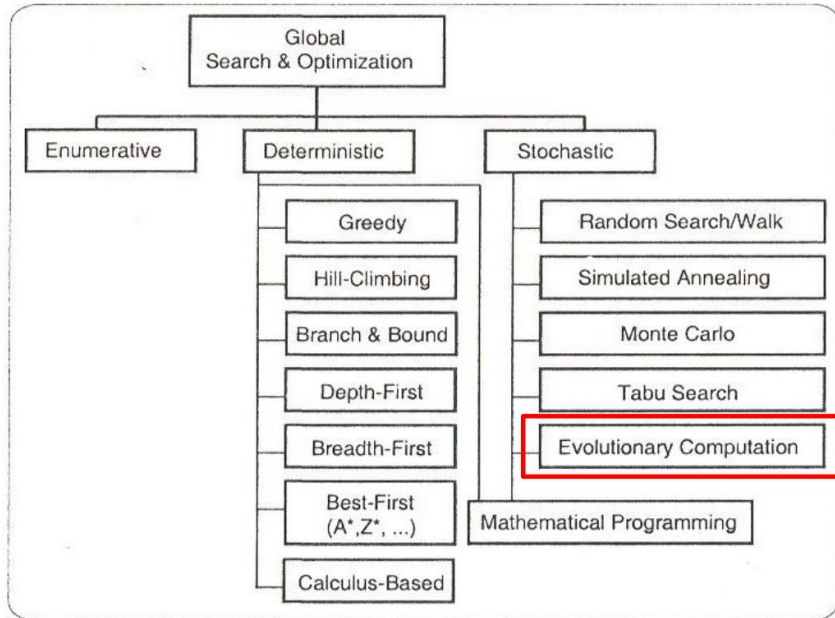


Figure 4.14: Global Optimization Approaches

Genetic Algorithm (GA) is an Evolutionary Computational concept optimization approach which is used to solve the complex optimization problems which need to be performed using the parallel search method based on the natural selection and general-purpose stochastic method. [14] According to the several literature surveys, the Genetic Algorithm is an intelligent and efficient optimization process. This algorithm is initiated with the basics of the Generation Evolutionary Concept. This algorithm is a kind of examination of Natural Adaptation Mechanisms and particularly suitable for the multidimensional global problems. This Algorithm is especially useful when there are multiple local minimums available in a specific search space.

This algorithm measures the fitness of each variable and then selects the best individual which best fits the given conditions. This algorithm implementation having four stages. The first one is randomly initializing the population called chromosomes

(initial Population). Secondly evaluate the fitness of the chromosome population (evaluation function). Third one is selecting the best individual using reproduction technique (selection). Finally manipulate the chromosomes using genetic rules towards the best fitness (genetic operators like crossover and mutation). [14] This process repeats until achieving the best solution or other stopping criteria.

#### 4.4.3. Algorithm Development

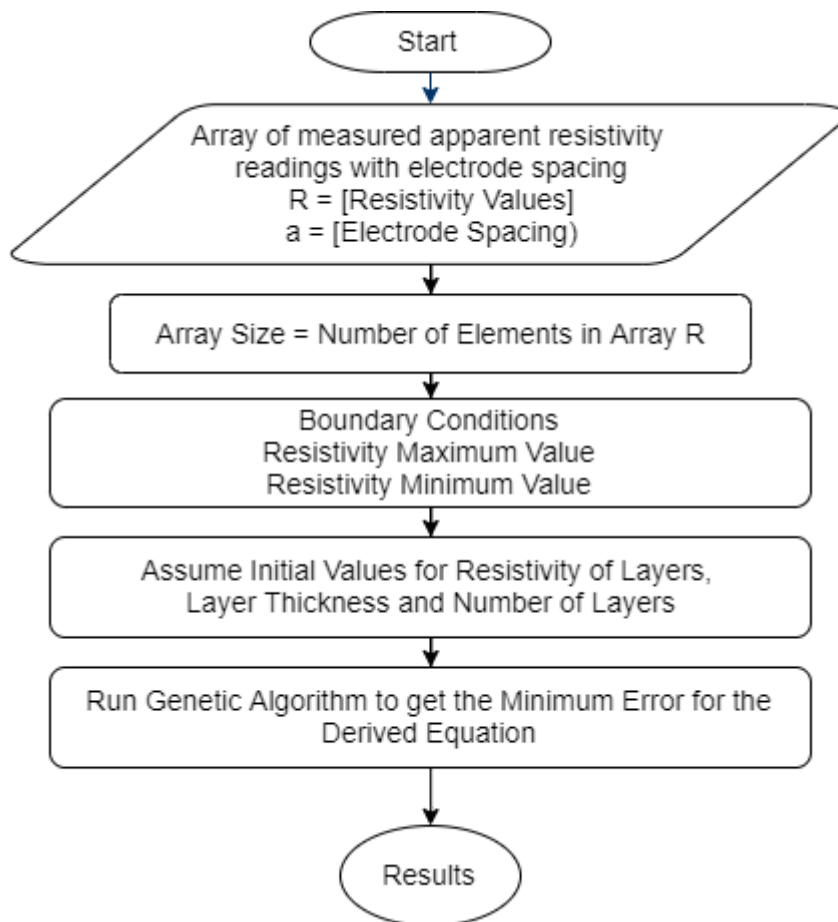


Figure 4.15: Data Acquisition of the Algorithm

Optimization solver technique is defined as “ga” (Genetic Algorithm). It is processed on the MATLAB script optimization function called `err_fun_1.m`. The number of soil layers is fixed to six numbers. Number of variables defined as 11. Since five number of layer thickness and six number of layer average resistivity. The boundary conditions of layer thickness are defined as 1 m to 10 m and the layer average resistivity as  $1\Omega\text{m}$

to 20,000Ωm. Population initialization range “0 to 10000”, Population size “100”, reproduction, stopping criteria, fitness function “Stochastic Uniform”, fitness scaling “rank”, mutation “Gaussian”, crossover “Scattered”, migration “Forward”.

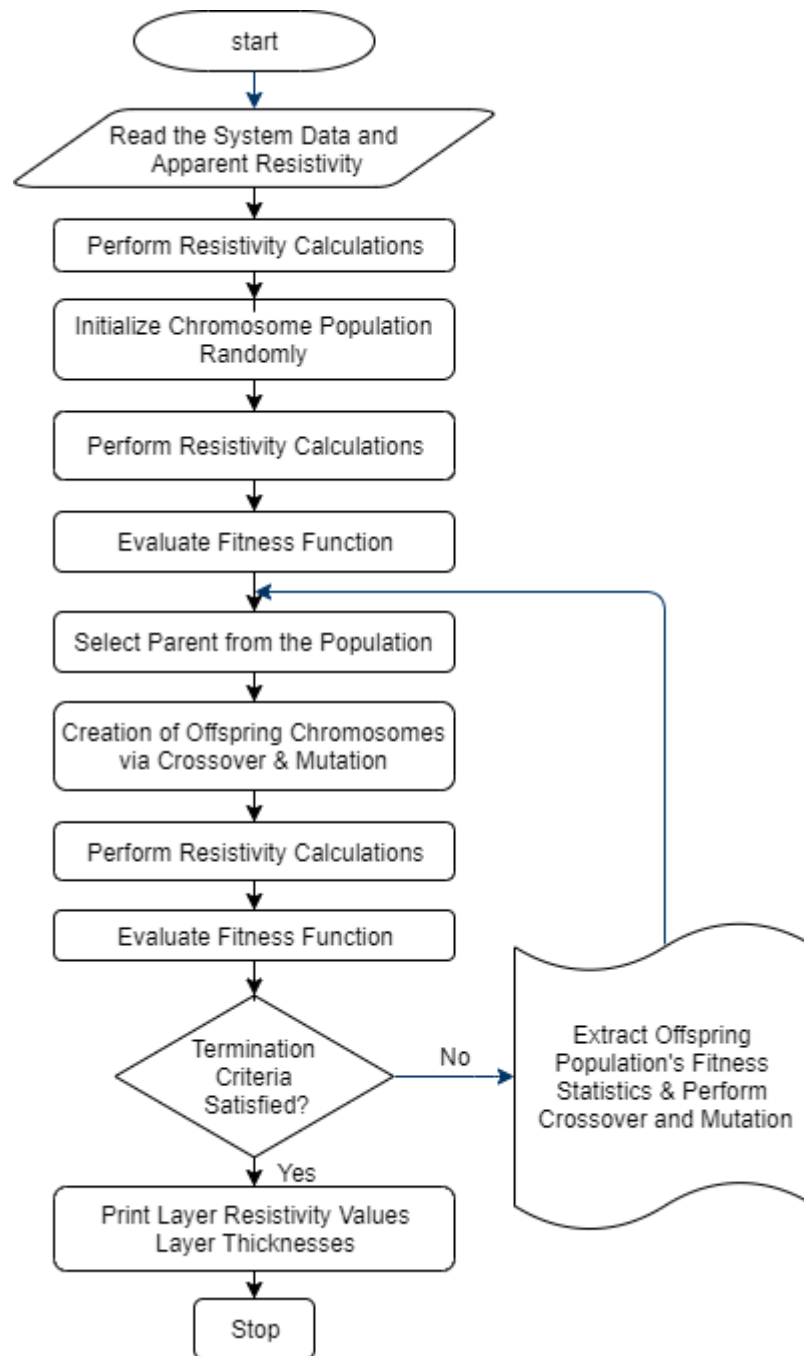


Figure 4.16: Flowchart of GA evaluation process for the proposed framework

### 5. FIELD MEASUREMENTS

There are two number of locations selected for the research. Location One is a 10 MW Solar power plant premises located in Vavuniya, Sri Lanka. Location Two is a 20 MW Wind Power Plant Location in Palai, Kilinichchi, Sri Lanka.

Earth resistance measurements were taken by GOSSEN METRAWATT GEOHM 5 Digital Earth Resistance Meter which is supporting Wenner Four- Probe Method



Figure 5.1: Digital Earth Resistance Meter GEOHM 5

#### 5.1. Preliminary Test

First, preliminary measurements were taken to analyze the sample data. This preliminary survey conducted to identify the shortcoming in the data analysis. The table 5.1 shows those preliminary readings. Measurements were taken by changing the distance between probes from 1 m to 5 m.

Table 5.1: Resistivity Measurements

Direction	Distance Between Probes				
	1	2	3	4	5
North	23.52	49	68.78	85.84	82.4
East	66.44	115.3	111.4	95.46	86.08
South	65.64	143.36	250	309	315.2
West	32.74	59.36	70.72	67.72	60

These measurements were taken from a single point to all four directions by changing the probe distances. The figure 5.2 shows the apparent resistivity variation

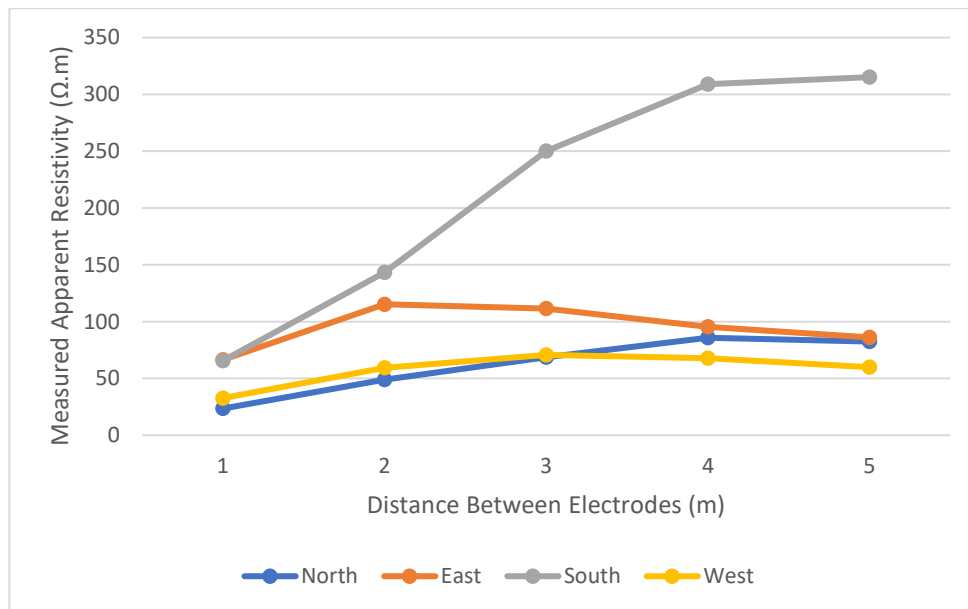


Figure 5.2: Apparent Resistivity ( $\rho_a$ ) vs distance between the electrodes

From the readings the large resistivity variations with directions can be clearly identified. Since these readings are taken from a single point, the south direction readings show an extremely high resistivity compared to all other directions when the probe spacing increases. So, from this preliminary survey can conclude that single point readings are not enough to do an accurate 3 D soil resistivity modelling.

## 5.2. Earth Resistivity Measurement Plan

### 5.2.1. Wenner Four Probe Measurement Plan

There is a 16 m x 16 m area land plot selected and the array of earth resistivity readings are taken and used for the accurate 3 D Soil Resistivity Modelling.

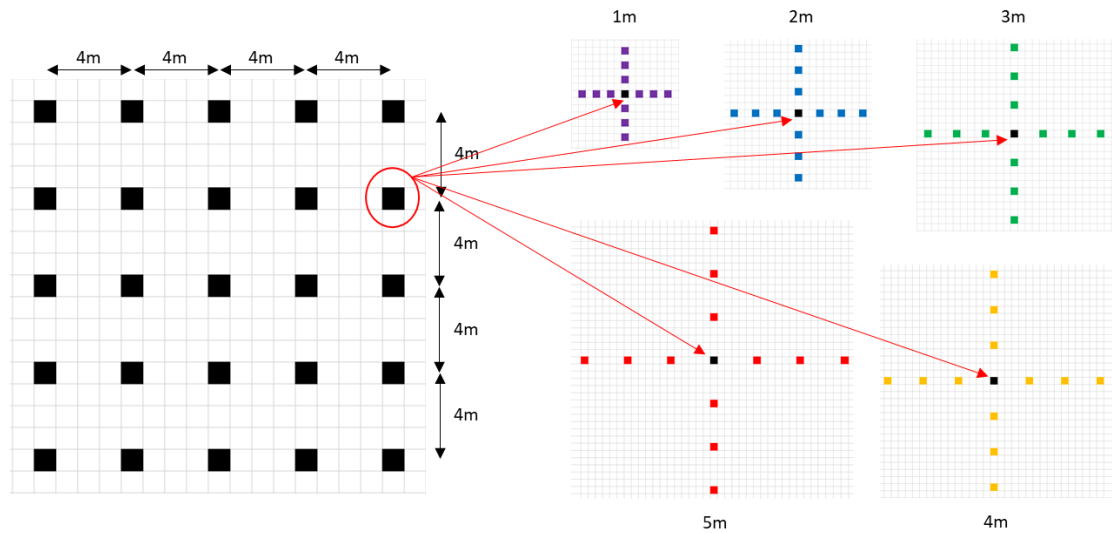


Figure 5.3: Apparent Earth Resistivity Reading Measurement Plan

There are 25 number of measurement points and 20 number of readings were taken from each point in all four directions.

### 5.2.2. Topsoil Measurement Plan

To increase the accuracy of this model, the topsoil resistivity is measured separately using the following method

The Box filled with the soil with the same compaction available in nature. The soil is removed from the top layer by measuring the same dimension of the box to confirm the same compaction level. DC Current is given through the two ends A, B and the

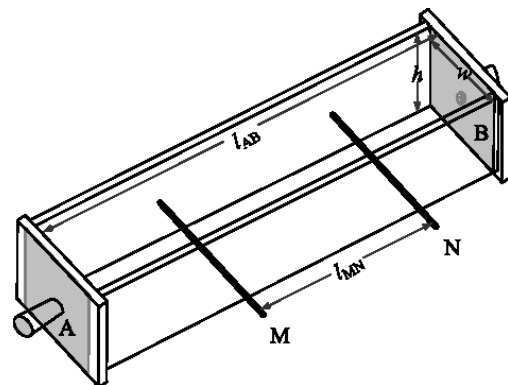


Figure 5.4: Soil box for soil resistivity measurement



voltage drop between M, N are measured. These measurements are used to calculate the resistivity.



Figure 5.5: Created Soil box for soil resistivity measurement

This soil box is made with plastic. Both ends having copper plates to inject the current into the soil. There are two number of rods in the middle which is used to measure the voltage drop.

### 5.3. Location 1

A flat land plot inside the 10 MW Solar Power Plant is selected for the first field measurements. It is a large flat land on the top and having boulders very close to the topsoil.



Figure 5.6: Selected area for the field measurement – Location 1



The selected area GPS coordinate is

Latitude N 8° 46' 9.852"

Longitude E 80° 31' 40.388"

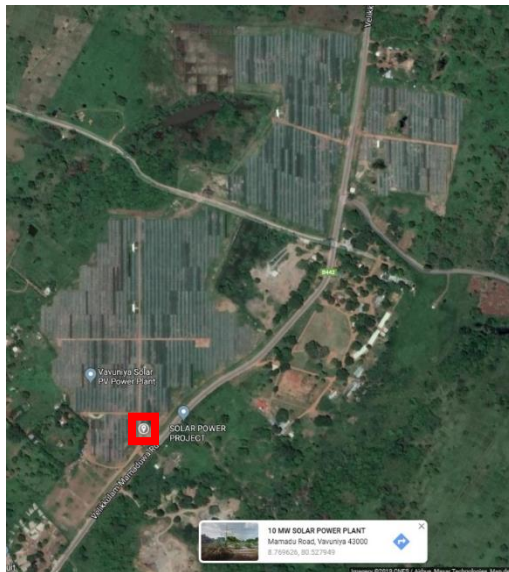


Figure 5.7: Selected area on the map

### 5.3.1. Earth Resistivity Wenner Method Measurements

Apparent earth resistivity measurements were taken using GOSSSEN METRAWATT GEOHM 5 Digital Earth Resistance Meter. It supports the Wenner four probe method to take apparent earth resistivity measurements.



Figure 5.8: Earth Resistivity Measurement



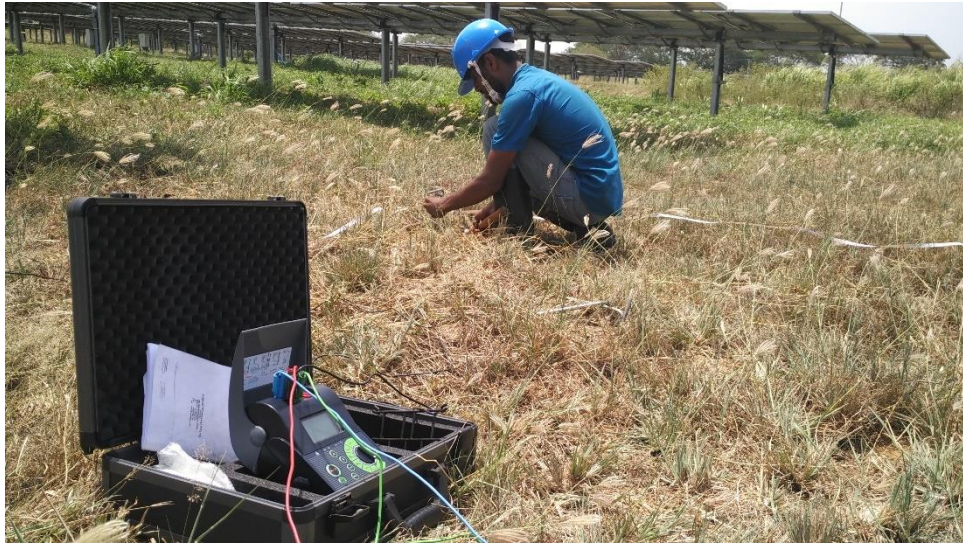


Figure 5.9: Earth Resistivity Measurement



Figure 5.10: Earth Resistivity probe arrangement – Location 1

There are around 150 earth probes used for this field measurements. All the earth probes are having same dimension and buried into the earth vertically with the same depth. The earth electrodes were arranged in a mesh grid to take all the probe spacing

readings for selected 25 locations within that mesh grid area. All the earth resistivity readings taken from the Digital earth resistivity meter is given in Table 5.2.

Table 5.2: Apparent Earth Resistivity Readings – Location 1

		1	2	3	4	5			1	2	3	4	5
1	W						2	W	43.1	45.7	47.8		
	N	47.9	51.8	49.8	40.7	37.8		N	75.3	78	72.9	65.6	68.2
	E	41.1	55.5	62.7	64.4	62		E	47.6	53.9	55.3	59.9	57.1
	S							S					
		1	2	3	4	5			1	2	3	4	5
3	W	43.8	58.8	57.6	42.7		4	W	33.4	44.9	56.4	64.7	48.7
	N	39.2	58.1	66	81.3	86.1		N	35.9	62	76.9	75.3	71.8
	E	33.4	45.8	53.3	53.5			E	29.6	50.9	53.1		
	S							S					
		1	2	3	4	5			1	2	3	4	5
5	W	30.4	42.4	53.4	59.6	62.9	6	W					
	N	51.7	72.5	69.2	55	65.7		N	36.1	43.2	50.5	49.4	46.4
	E							E	47.4	77.8	84.4	76.7	63
	S							S	45	53.5	65.7		
		1	2	3	4	5			1	2	3	4	5
7	W	54.2	46.6	57.2			8	W	48	69.3	79.1	63.7	
	N	55.1	75.2	78.6	80.3	69.4		N	55.3	70.1	86.2	66.1	67
	E	57.7	71.4	79.8	71.2	71.3		E	49	76.4	76.4	76.4	
	S	69	70.7	50.3				S	41.7	53.9	66.9		
		1	2	3	4	5			1	2	3	4	5
9	W	47.5	63.3	70.3	76.1	64.9	10	W	74.1	69.5	67.4	71.5	61.6
	N	54.1	60.7	55.8	68.1	79.6		N	48.3	58.2	74.7	80.6	87.2
	E	80.4	78.9	63.9				E					
	S	41.7	53.9	66.9				S	63.5	50.1	60.9		
		1	2	3	4	5			1	2	3	4	5
11	W						12	W	53	60.9	54.2		
	N	43.6	46.1	43.3	36.8			N	48	60.7	57.9	55.5	
	E	46.3	56.2	69.3	69.9	71.2		E	48.9	63.8	70.9	75.5	65.6
	S	29.6	50.5	53.2	66.1			S	55	77.6	80.2	84.4	

		1	2	3	4	5
13	W	61.1	80.7	70.2	58.7	
	N	39.7	50.8	54.4	71.3	
	E	43	56.1	57.1	59	
	S	66.9	63.8	56	65	

		1	2	3	4	5
14	W	41.4	67.3	71.7	70.9	58.7
	N	37.1	55.2	67	74.6	
	E	39.2	55.5	63.1		
	S	66.9	63.8	56	65	

		1	2	3	4	5
15	W	39.5	50.3	59.3	68.9	71.9
	N	59.5	65.8	65.3	74.2	
	E					
	S	35.2	52.9	69	69.1	

		1	2	3	4	5
16	W					
	N	39.1	40.5	31.9		
	E	50.4	60	61.7	58.4	55.6
	S	46.1	53	49.2	39.8	45.8

		1	2	3	4	5
17	W	51.2	41	52.7		
	N	33.3	39.5	50.7		
	E	32.9	50.8	61.2	72.1	78.6
	S	55.8	71.7	79.1	62.5	68.1

		1	2	3	4	5
18	W	27.1	48.9	58.6	57.8	
	N	32.2	49.9	71.6		
	E	39	58.6	71.9	75.8	
	S	36.8	60.9	79.9	80.8	70.3

		1	2	3	4	5
19	W	37.8	51.6	57.9	62	54.7
	N	41.6	56.8	75.9		
	E	48.3	62.4	68.9		
	S	41	53.4	59.5	69.7	77.4

		1	2	3	4	5
20	W	46.9	60.9	65.3	69.7	65.5
	N	55.5	72.5	77.3		
	E					
	S	53.1	54.5	51.5	51.6	59

		1	2	3	4	5
21	W					
	N					
	E	24.9	35.9	44.7	62.7	63.1
	S	31	44.8	44.3	50.4	41.2

		1	2	3	4	5
22	W	23.6	24.8	41.4		
	N					
	E	33.4	44.6	60.2	63.8	77.4
	S	29	49.6	63.5	80.4	70.2

		1	2	3	4	5
23	W	29.2	37.8	39.4	41.4	
	N					
	E	35.5	41.5	50.6	84.5	
	S	30.3	48.6	59.6	64.2	81.5

		1	2	3	4	5
24	W	34.4	48.2	57.7	60.8	53.9
	N					
	E	64.3	74.5	72.8		
	S	41.5	59.4	73.4	69.6	68.1

		1	2	3	4	5
25	W	59.1	66.9	61.5	62	62.2
	N					
	E					
	S	55.2	64.7	68.1	79.8	70.9



### 5.3.2. Topsoil Resistivity Measurements

Topsoil Resistivity is measured using the separate method. It assumed that the topsoil parameters within the measurement area is uniform. One location within the mesh grid is selected and the same measurement of the soil box quantity soil area is cut and filled to confirm the same compaction level exists in the nature.



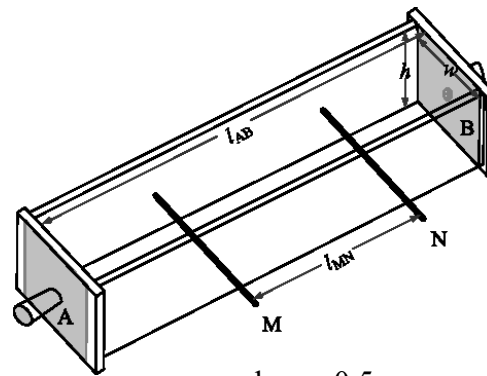
Figure 5.11: Topsoil excavation and soil box filling



Figure 5.12: Soil box testing for location 1

Table 5.3: Soil box Measurements

Current (A)	Voltage (V)
0.0029	10
0.0059	20.3
0.0087	30
0.0116	40.1
0.0146	50
0.0176	60
0.0207	70
0.0239	80
0.0301	101.4

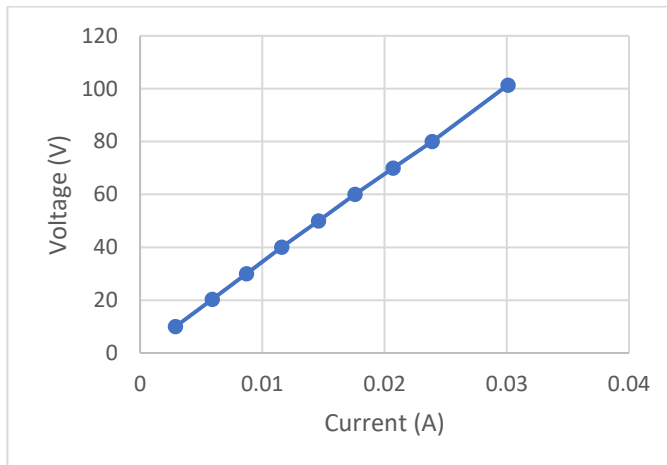


$$l_{MN} = 0.5 \text{ m}$$

$$h = 0.15 \text{ m}$$

$$w = 0.15 \text{ m}$$

Figure 5.13: Soil box dimensions



$$R_{MN} = V_{MN}/I_{MN}$$

$$R_{MN} = 3,368.8 \ \Omega$$

$$R_{MN} = \rho \times L_{MN}/A$$

$$\rho = R_{MN} \times A / L_{MN}$$

$$\rho = 3,368.8 \times 0.15^2 / 0.5 \ \Omega\text{m}$$

$$\rho = 151.59 \ \Omega\text{m}$$

Figure 5.14: Soil box Readings

The topsoil is showing considerably high value compared to the apparent earth resistivity measurements. There can be low resistivity soil layers at the bottom of the topsoil layer. Also, there is a possibility of inadequate compaction level inside the soil box compared to the soil compaction exist in nature

#### 5.4. Location 2

A flat land plot inside the 20 MW Wind Power Plant is selected for the first field measurements. It is a large flat land very close to sea.



Figure 5.15: Selected area for the field measurement – Location 2

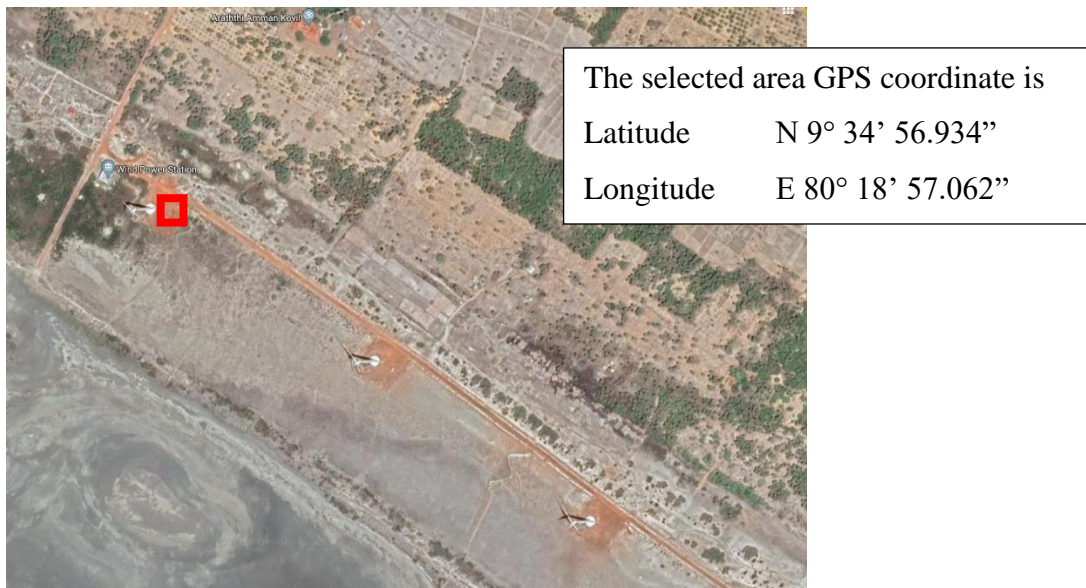


Figure 5.16: Selected area on the map



#### 5.4.1. Earth Resistivity Wenner Method Measurements

Apparent earth resistivity measurements were taken using GOSSEN METRAWATT GEOHM 5 Digital Earth Resistance Meter. It supports the Wenner four probe method to take apparent earth resistivity measurements.



Figure 5.17: Earth Resistivity Measurement



Figure 5.18: Earth Resistivity probe arrangement – Location 2

There are around 150 earth probes used for this field measurements. All the earth probes are having same dimension and buried into the earth vertically with the same depth. The earth electrodes were arranged in a mesh grid to take all the probe spacing



readings for selected 25 locations within that mesh grid area. All the earth resistivity readings taken from the Digital earth resistivity meter is given in Table 5.4.

Table 5.4: Apparent Earth Resistivity Readings – Location 2

		1	2	3	4	5			1	2	3	4	5
1	W						2	W	7.88	6.3	6.32		
	N	5.1	6.32	7.83	7.14	8.96		N	8.8	7.32	6.94	7.33	7.07
	E	5.18	5.9	6.42	7.39	6.69		E	6.12	5.93	5.7	5.55	6.97
	S							S					
		1	2	3	4	5			1	2	3	4	5
3	W	6.03	5.98	6.67	7.18		4	W	4.12	5.63	6.17	6.04	7.28
	N	4.65	5.9	5.67	7.45	8.33		N	3.96	5.9	6.34	6.77	6.92
	E	5.18	5.19	5.47	6.26			E	4.41	4.93	5.7		
	S							S					
		1	2	3	4	5			1	2	3	4	5
5	W	4.37	4.81	5.7	6.9	6.75	6	W					
	N	4.61	5.16	5.46	6.19	6.29		N	7.22	6.38	6	7.24	8.4
	E							E	9.04	6.91	7.59	6.95	6.85
	S							S	6.11	5.75	6.45		
		1	2	3	4	5			1	2	3	4	5
7	W	6.45	7.31	7.11			8	W	6.11	6.61	7.23	8.13	
	N	8.02	7.57	7.15	7.37	8.13		N	2.07	7.22	7.78	6.96	7.17
	E	7.91	8.32	6.91	6.74	8.06		E	4.59	6.43	6.54	7.68	
	S							S	4.49	5.48	6.61		
		1	2	3	4	5			1	2	3	4	5
9	W	6.2	5.17	7.78	6.8	7.79	10	W	4.35	5.45	6.71	6.46	7.98
	N	5.58	6.43	4.76	6.85	6.46		N	5.25	5.6	5.48	7.08	7
	E	5.25	4.65	6.21				E					
	S	4.73	4.73	4.17				S	4.49	5.54	5.86		
		1	2	3	4	5			1	2	3	4	5
11	W						12	W	6.38	7.26	7.35		
	N	7.3	6.84	8.45	6.01			N	7.05	7.42	7.28	7.65	
	E	7.09	7.65	7.83	7.89	7.59		E	7.15	7	6.74	6.22	7.24
	S	7.63	7.27	6.56	6.16			S	7.68	7.4	6.77	7.22	

		1	2	3	4	5
13	W	6.41	6.47	9.09	7.49	
	N	6.54	7.04	7.07	7.61	
	E	6.22	6.89	6.07	6.54	
	S	5.66	5.96	6	6.62	

		1	2	3	4	5
14	W	6.27	6.36	6.98	6.79	6.61
	N	5.62	6.85	6.07	6.66	
	E	5.71	6.16	6.14		
	S	5.22	2.06	6.59	6.91	

		1	2	3	4	5
15	W	4.97	5.79	7.68	7.57	7.75
	N	4.8	6.64	6.99	6.13	
	E					
	S	5.64	5.73	5.63	6.28	

		1	2	3	4	5
16	W					
	N	7.83	6.07	5.79		
	E	6.86	7.48	7.96	7.66	6.87
	S	6.74	7.78	8.09	8.37	6.9

		1	2	3	4	5
17	W	6.88	7.29	7.73		
	N	7.05	7.36	7.24		
	E	7.66	7.04	7.02	6.9	6.1
	S	6.81	6.95	7.77	7.11	7.57

		1	2	3	4	5
18	W	6.61	7.33	6.77	7.52	
	N	6.23	7.1	6.76		
	E	6.17	6.97	6.44	7.05	
	S	6.37	6.45	6.88	6.91	7.77

		1	2	3	4	5
19	W	6.56	6.87	6.65	7.36	7.68
	N	6.42	6.5	6.85		
	E	6.07	6.83	6.57		
	S	5.62	5.96	5.14	6.72	6.55

		1	2	3	4	5
20	W	6.2	6.01	6.73	6.86	7.27
	N	5.56	5.77	6.77		
	E					
	S	6.2	6.03	7.22	6.73	8.65

		1	2	3	4	5
21	W					
	N					
	E	6.68	6.6	7.28	7.72	5.52
	S	6.63	8.25	7.2	7.16	8.15

		1	2	3	4	5
22	W	6.48	7.57	7.34		
	N					
	E	6.28	9.05	6.53	6.51	7.52
	S	6.71	7.06	7.12	7.52	7.68

		1	2	3	4	5
23	W	6.38	9.16	7.19	7.39	
	N					
	E	5.89	6.7	6.54	7.01	
	S	6.21	6.84	6.73	7.13	6.93

		1	2	3	4	5
24	W	5.75	6.49	6.01	6.69	7.87
	N					
	E	5.93	6.65	6.93		
	S	5.75	6.56	6.36	6.78	6.24

		1	2	3	4	5
25	W	5.93	6.57	6.72	6.79	7.28
	N					
	E					
	S	5.33	5.74	6.62	7.1	9.21

#### 5.4.1. Top Soil Resistivity Measurements

Topsoil Resistivity is measured using the separate method. It assumed that the topsoil parameters within the measurement area is uniform. One location within the mesh grid is selected and the same measurement of the soil box quantity soil area is cut and filled to conform the same compaction level exists in the nature.



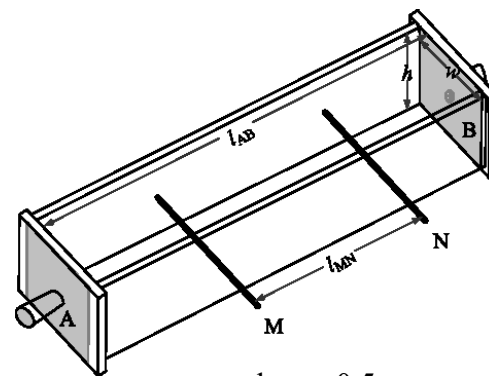
Figure 5.19: Top soil excavation and soil box filling



Figure 5.20: Soil box testing for location 2

Table 5.5: Soil box Measurements

Current (A)	Voltage (V)
0.198	10.45
0.389	20.5
0.5865	30.7
0.7749	40.4
0.9715	50.3
1.1745	60.3

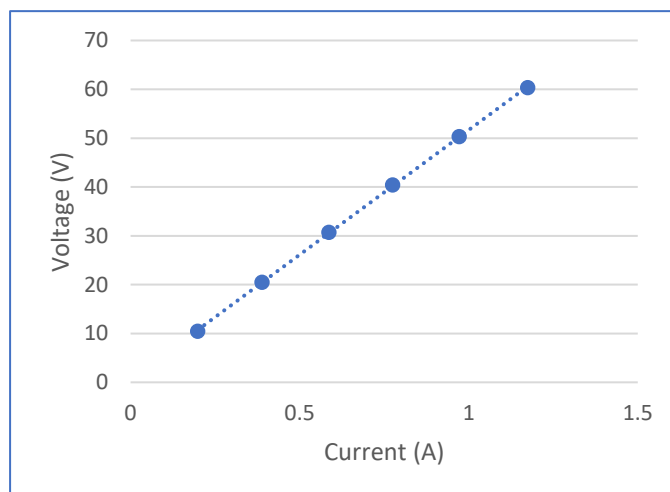


$$l_{MN} = 0.5 \text{ m}$$

$$h = 0.15 \text{ m}$$

$$w = 0.15 \text{ m}$$

Figure 5.21: Soil box dimensions



$$R_{MN} = V_{MN}/I_{MN}$$

$$R_{MN} = 51.34 \text{ } \Omega$$

$$R_{MN} = \rho \times L_{MN}/A$$

$$\rho = R_{MN} \times A / L_{MN}$$

$$\rho = 51.34 \times 0.15^2 / 0.5 \text{ } \Omega\text{m}$$

$$\rho = 2.31 \text{ } \Omega\text{m}$$

Figure 5.22: Soil box Readings

The topsoil shows a very low resistivity value. This location is 500 m away from the sea water. So, the salinity level of the topsoil is high. This can be the reason for the low resistivity value. All the apparent resistivity values are higher than the top layer resistivity. Which shows the bottom layers having considerably higher resistivities compared to the topsoil layer.

6. ANALYTICAL RESULTS

6.1. Measurements

There are around 350 readings were taken per location. Total 25 measurement points per location in 16 m x 16 m square area. Those 25 points resistivity measurements are taken from all four direction and probe spacing 1 m to 5 m.

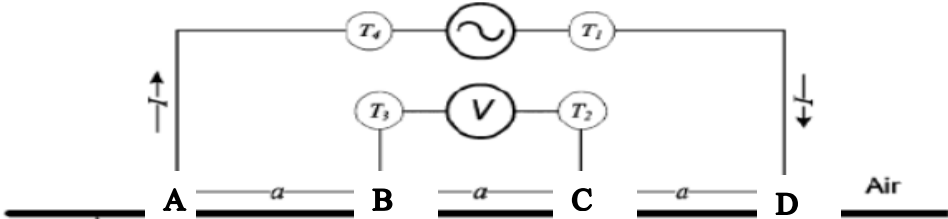


Figure 6.1: Wenner four probe earth resistivity measurement method

If the measurement point is A, the actual apparent resistivity reading will be the average resistivity of the soil between the voltage probes. So, the real point will be in a distance of  $3a/2$  from the actual base measurement point. By considering this, the actual reading points will as be shown in Figure 6.2 – Figure 6.6.

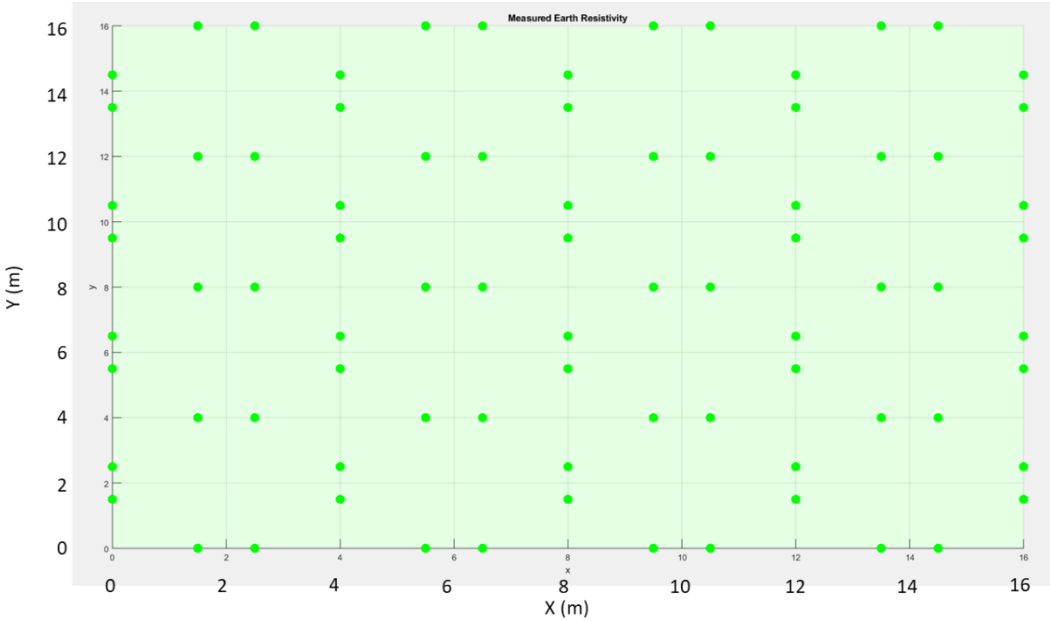


Figure 6.2: 1 m Probe Spacing Data Coordinates

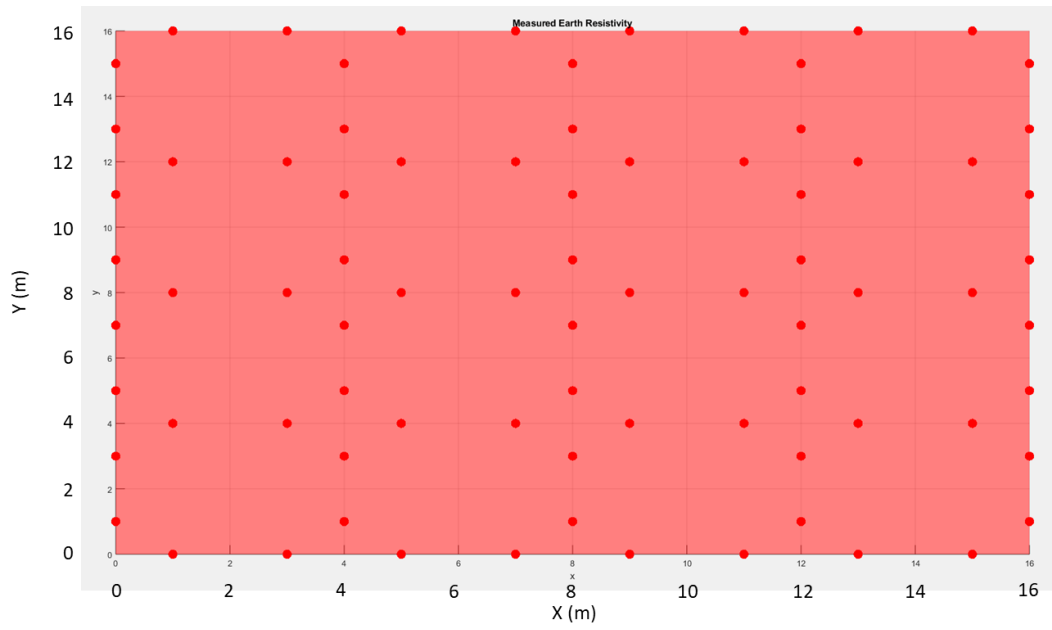


Figure 6.3: 2 m Probe Spacing Data Coordinates

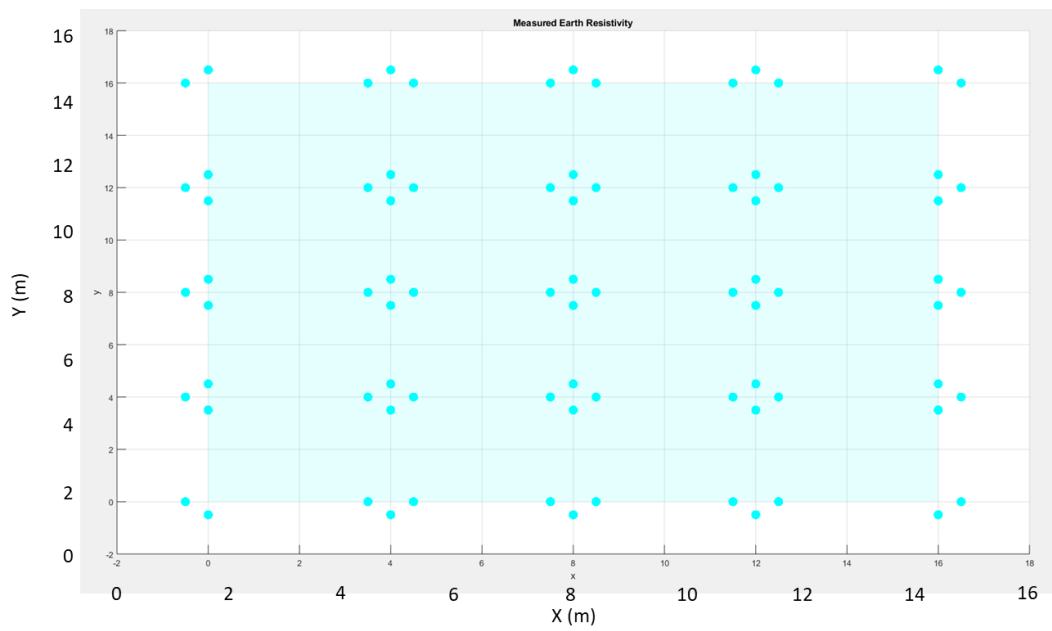


Figure 6.4: 3 m Probe Spacing Data Coordinates

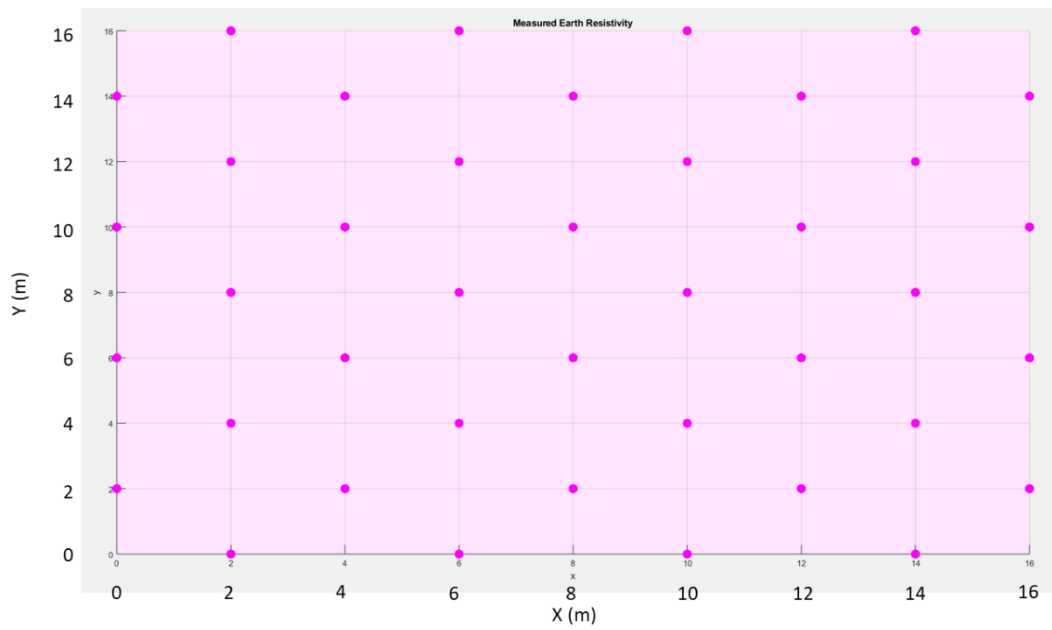


Figure 6.5: 4 m Probe Spacing Data Coordinates

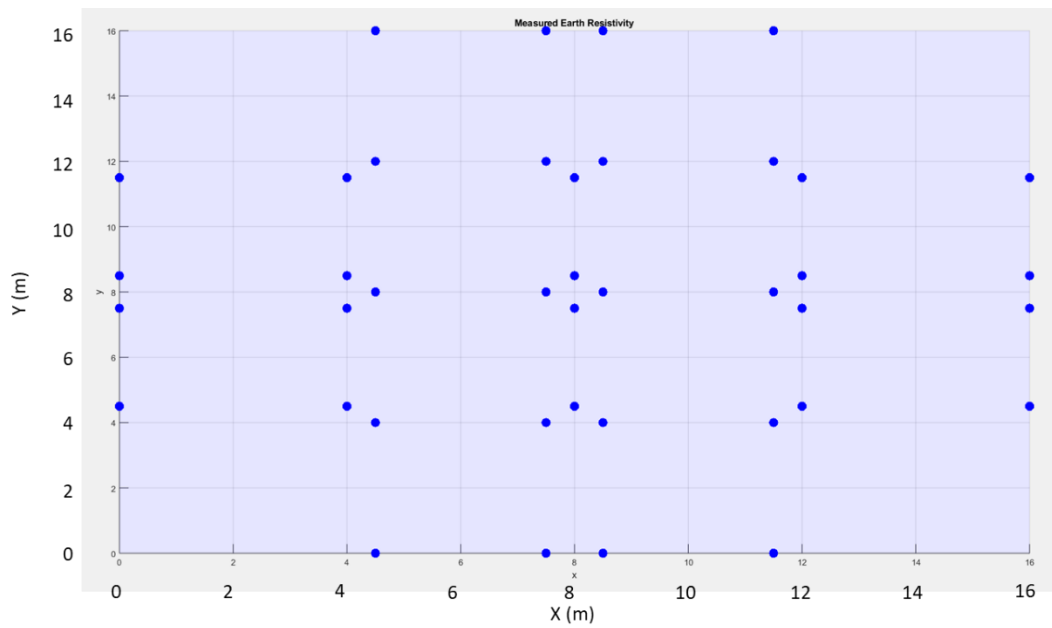


Figure 6.6: 5 m Probe Spacing Data Coordinates

## 6.2. Location 1 - 10 MW Solar Power Plant - Vavuniya

Each reading plotted according to the probe spacings separately. Scattered points interpolated and extrapolated and plotted separately.

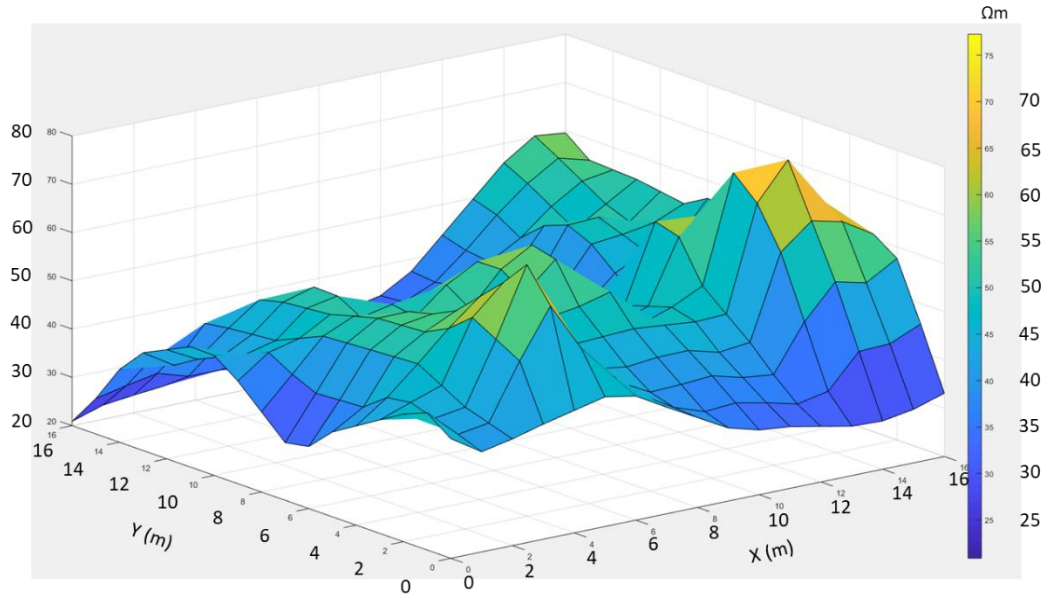


Figure 6.7: 1 m Probe Spacing Resistivity Data Plot

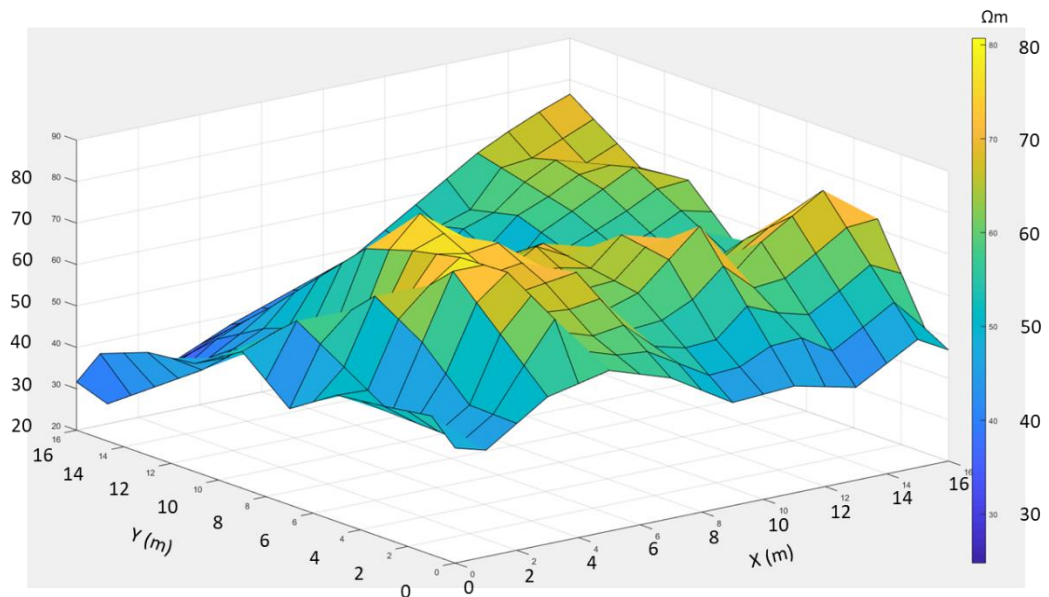


Figure 6.8: 2 m Probe Spacing Resistivity Data Plot



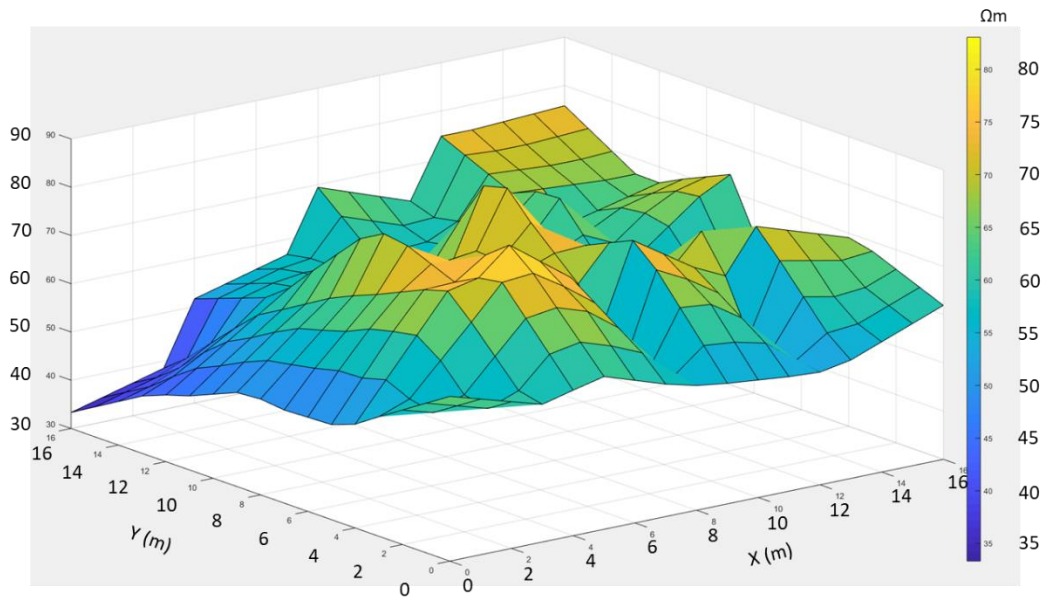


Figure 6.9: 3 m Probe Spacing Resistivity Data Plot

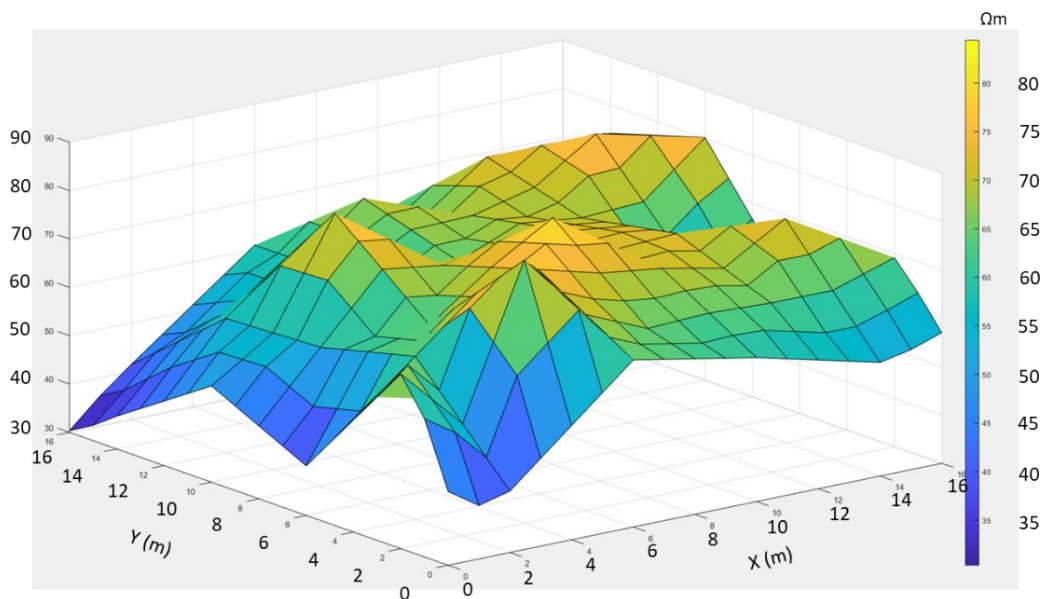


Figure 6.10: 4 m Probe Spacing Resistivity Data Plot

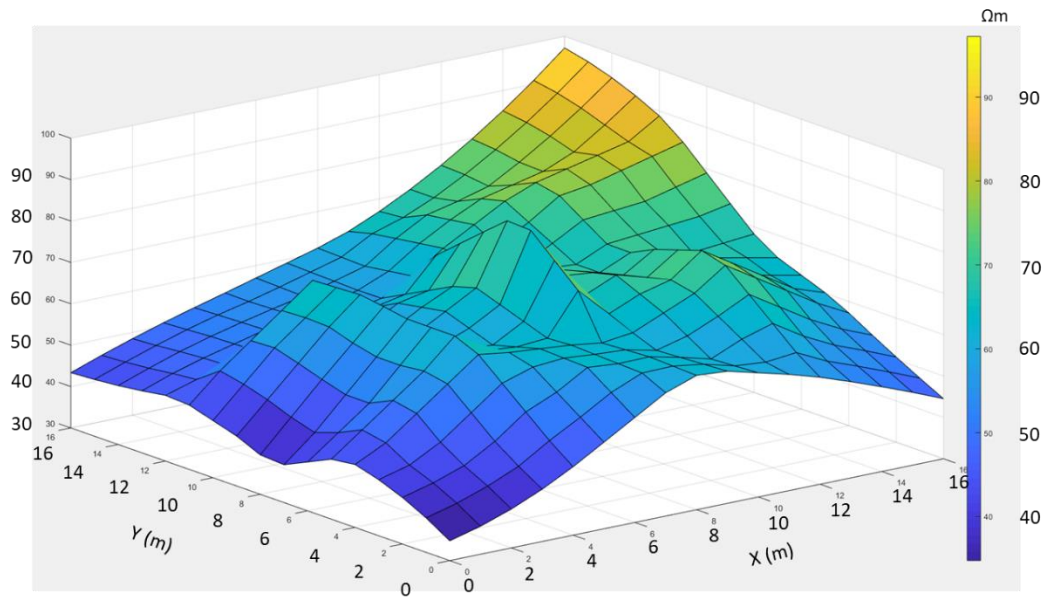


Figure 6.11: 5 m Probe Spacing Resistivity Data Plot

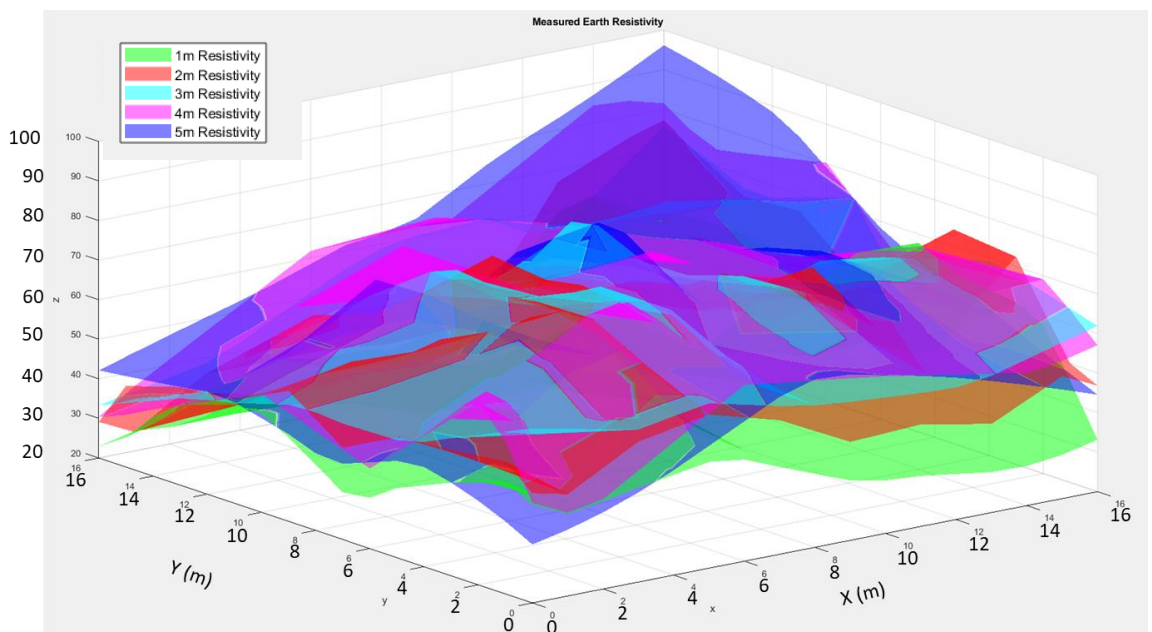


Figure 6.12: All Probe Spacing Resistivity Readings Data Plot – Location 1

From the interpolated and extrapolated resistivity data plot (Figure 6.12) the following apparent resistivity data were extracted for specific coordinates of Location 1 (10 MW Solar Power Plant in Vavuniya).

Table 6.1: Apparent Resistivity Readings from the Data Plot

X	Y	1m	2m	3m	4m	5m
0	0	44.7715	47.7251	64.1375	45.2271	34.7693
0	4	40.5500	51.1500	51.5000	53.1750	45.2043
0	8	36.6000	48.1000	49.8500	45.0750	39.5000
0	12	42.6000	45.4500	43.8000	43.3500	45.8598
0	16	22.9316	29.1018	33.3250	30.3498	42.1399
4	0	45.3500	57.1500	60.1500	53.6250	46.5223
4	4	62.0500	77.8000	76.5500	74.2250	65.6347
4	8	51.5000	73.4500	78.8500	72.2000	69.2000
4	12	44.5500	55.1500	60.7000	67.9250	53.7667
4	16	28.5000	36.8500	42.0500	51.5750	52.6602
8	0	38.6000	49.4000	55.8500	62.1500	62.4500
8	4	48.5000	60.9500	61.0000	73.0250	62.3000
8	8	53.3000	65.5000	83.0500	73.1000	83.8000
8	12	34.5000	49.7000	57.0000	68.2250	60.5500
8	16	32.3500	46.4000	58.9500	62.3250	62.6500
12	0	31.5000	44.1000	53.3500	56.6250	55.8497
12	4	47.9000	62.9000	66.4500	68.7500	74.8889
12	8	52.0000	57.0500	57.6500	70.6750	69.9500
12	12	41.3000	57.3000	70.2000	71.7250	79.4611
12	16	49.3500	54.2000	56.0500	73.7000	79.1951
16	0	33.1175	46.8420	61.9125	57.0270	44.5331
16	4	55.9000	62.7000	69.1000	61.2000	57.2465
16	8	47.3500	56.3500	63.1000	66.7500	68.3000
16	12	54.3000	65.2500	66.7000	77.2000	88.4909
16	16	53.8192	77.2701	75.8000	81.5349	96.1872

The apparent resistivity data with probe spacing shown in Table 6.1 is used as the input data for the analysis. Genetic Algorithm is used for the optimization.

Table 6.2: Final Results from the Genetic Algorithm Optimization

X	Y	P1	h1	P2	h2	P3	h3	P4	h4	P5	h5	P6
0	0	42.07	8.77	34.51	1.01	747.09	1.32	45.75	1.30	4587.59	1.00	1.06
0	4	4.94	1.03	8569.44	1.25	15.30	9.20	5034.21	1.68	6396.46	1.96	1206.87
0	8	22.19	4.72	1708.42	1.78	1.89	9.68	2775.17	7.16	6577.63	2.55	10995.67
0	12	44.63	9.97	6.33	2.79	14281.56	1.35	479.03	8.24	398.92	8.59	7847.01
0	16	18.89	7.77	44.19	1.31	14513.80	1.11	208.86	8.29	3261.17	1.00	2007.61
4	0	37.52	6.70	62.76	1.18	16914.67	1.00	15.09	8.68	12313.91	1.42	191.05
4	4	20.19	2.18	3314.87	1.53	552.59	0.80	1.21	0.98	9601.57	2.65	15043.89
4	8	20.23	3.40	16905.49	1.22	35.02	7.84	1191.90	4.13	7844.13	7.20	8568.09
4	12	19.11	5.16	16122.82	1.05	5970.59	1.43	5780.78	1.13	960.88	2.09	6.52
4	16	22.91	2.48	56.66	7.64	88.19	3.26	10418.76	1.30	385.83	5.98	3.69
8	0	14.69	4.96	19999.73	1.00	18457.82	1.25	13227.41	1.20	9491.49	1.24	358.02
8	4	34.74	7.49	1104.93	2.92	7056.57	1.00	0.98	5.54	1.01	5.85	1.05
8	8	33.11	6.50	6947.34	1.14	350.88	9.76	1771.31	1.01	3426.73	2.12	415.51
8	12	28.07	7.63	586.17	1.68	3198.45	2.24	0.84	7.53	12142.12	8.77	9027.24
8	16	24.02	5.71	139.37	1.00	4667.02	1.51	4138.49	1.55	254.30	2.73	79.33
12	0	17.38	5.34	3506.28	2.25	761.52	1.89	918.28	1.04	3897.12	1.23	1.04
12	4	23.87	4.24	7104.04	1.20	11.48	1.37	7839.47	1.06	10336.89	1.69	19991.83
12	8	31.01	7.67	8800.64	1.04	265.90	7.22	2412.33	2.93	680.83	5.37	1.00
12	12	21.90	5.96	9089.44	2.46	14555.92	1.01	1.00	2.36	17809.09	9.33	4673.83
12	16	27.67	6.19	5607.85	1.02	221.14	7.50	1611.47	4.20	10136.54	6.99	6091.04
16	0	30.70	6.65	65.85	1.02	5025.55	1.46	1.00	9.12	70.28	5.11	4080.52
16	4	40.95	1.00	75.26	9.60	365.83	1.59	53.63	1.00	1.96	7.78	10569.86
16	8	25.48	6.64	7596.02	1.70	60.87	7.61	2696.61	5.16	4085.77	1.11	11155.96
16	12	13.97	2.74	19856.34	0.94	17667.04	0.93	2205.18	1.02	195.61	6.16	3453.23
16	16	17.22	1.22	411.01	1.11	1454.08	1.00	29.89	5.13	1033.21	2.41	15406.66

Each layer thickness (h) and the average resistivity of that layer ( $\rho$ ) were optimized for the minimum error using Genetic Algorithm (GA). The number of layers were limited to six to reduce the process time. The last layer  $\rho_6$  is having an infinity layer height. Table 6.4 shows the processed data using GA. This data is used to plot the three-dimensional model of the measured soil area.



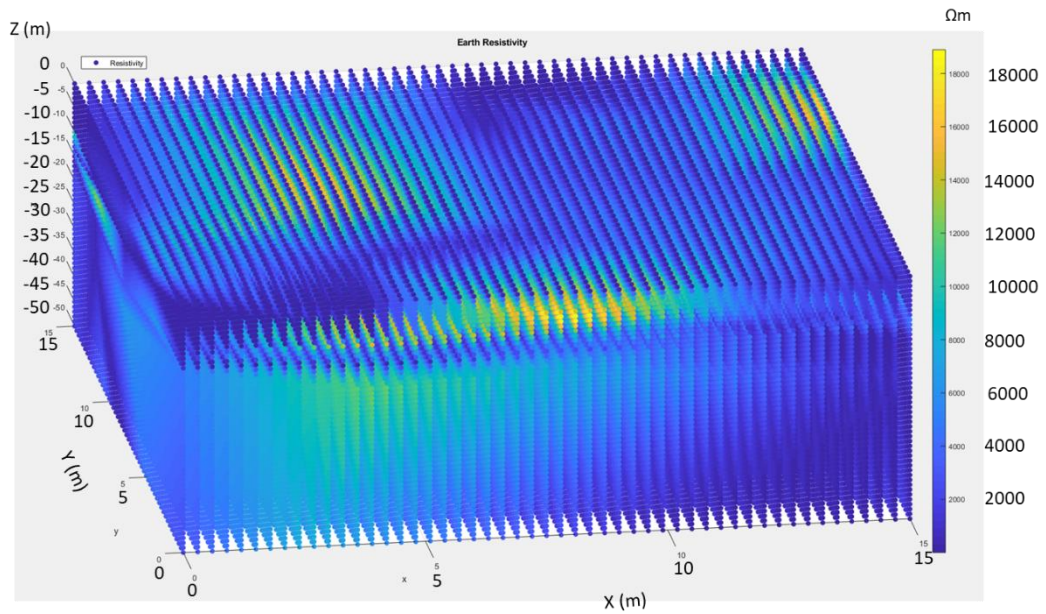


Figure 6.13: Final Results- 3 D Modelling of Earth Resistivity for Location 1

### 6.2.1. Results Validation

There are two test locations selected from the graph. One is with the high resistivity zone near to the earth surface. Other location is normal.

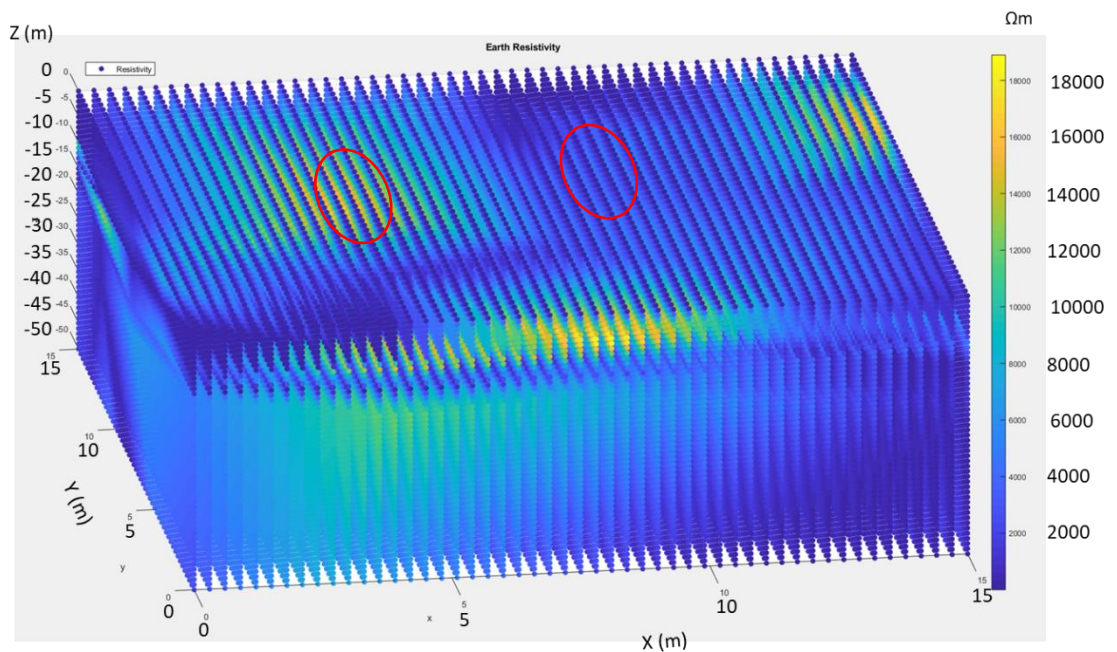


Figure 6.14: Borehole Locations

Both of those location coordinates were physically marked in the real ground and two boreholes were excavated in those locations to conform the reason for the soil resistivity variations.



Figure 6.15: Borehole excavation

Borehole location 1 is selected in the coordinate of (4,8). Which is having high variation of earth resistivity near to the topsoil.

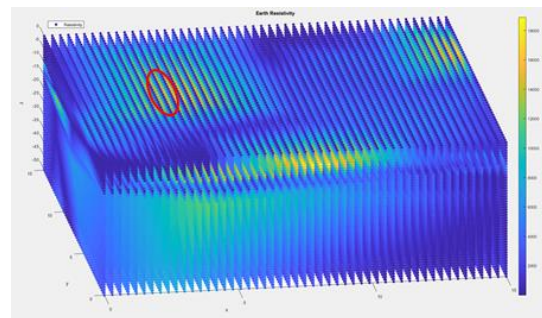


Figure 6.16: Borehole Location 1



Figure 6.17: Rock at 2m Depth



Figure 6.18: Rock Sample from the Large Bed Rock

There is a bedrock found at 2 m depth from the topsoil.



Borehole location 2 is selected in the coordinate of (8,8). Which is not having any variation in the earth resistivity near to the topsoil.

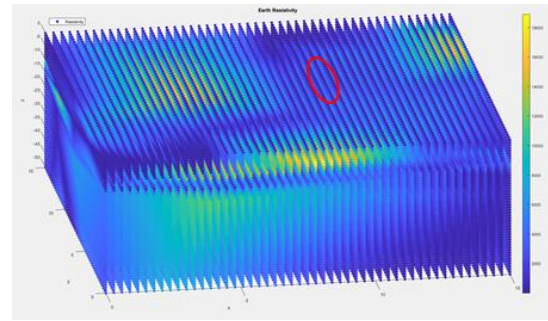


Figure 6.19: Borehole Location 2



Figure 6.20: Borehole up to 3.5 m

There are not rocks found up to 3.5 m depth from the topsoil.

Borehole Location 1 have a high resistivity starts from 3 m depth according to the three-dimensional model. But in real case, that location having rocks at 2 m depth. Also, borehole location 2 not having any rock layer at the bottom. There is no rock found when that location excavated. Can conclude from this results that this model giving the result with a certain accuracy. The accuracy needs to be improved further. This is discussed in the limitation section of this report.

### 6.3. Location 2 - 20 MW Wind Power Plant - Kilinichchi

Each earth resistivity readings plotted according to the probe spacings separately. Scattered points were interpolated and extrapolated to find the grid of apparent resistivity values and plotted separately.

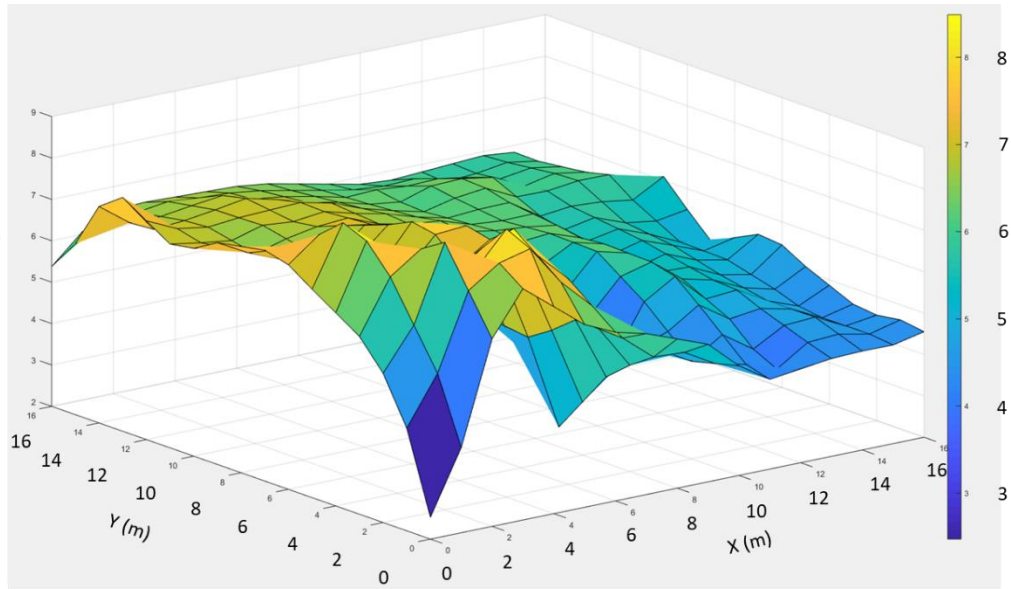


Figure 6.21: 1 m Probe Spacing Resistivity Data Plot

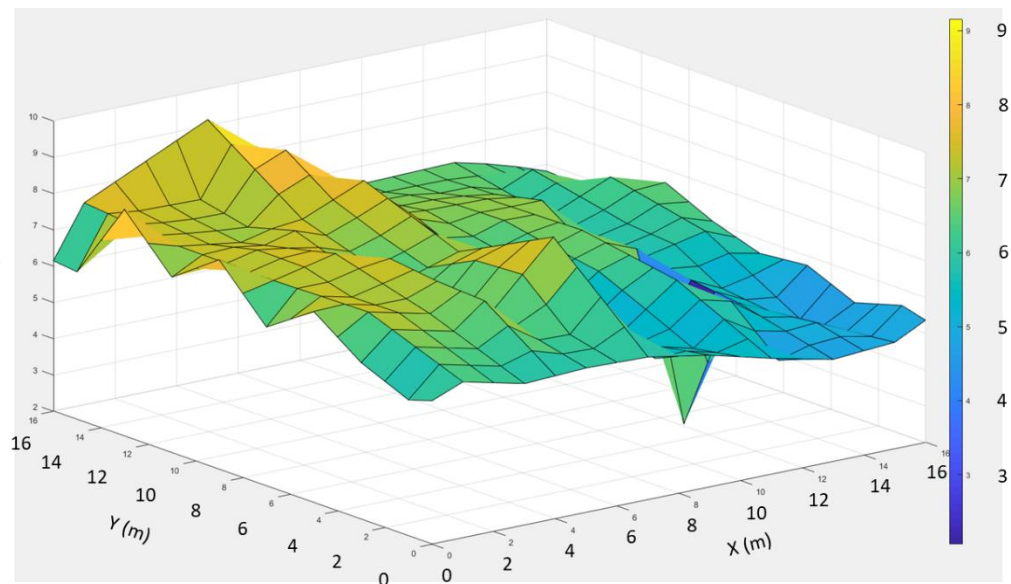


Figure 6.22: 2 m Probe Spacing Resistivity Data Plot



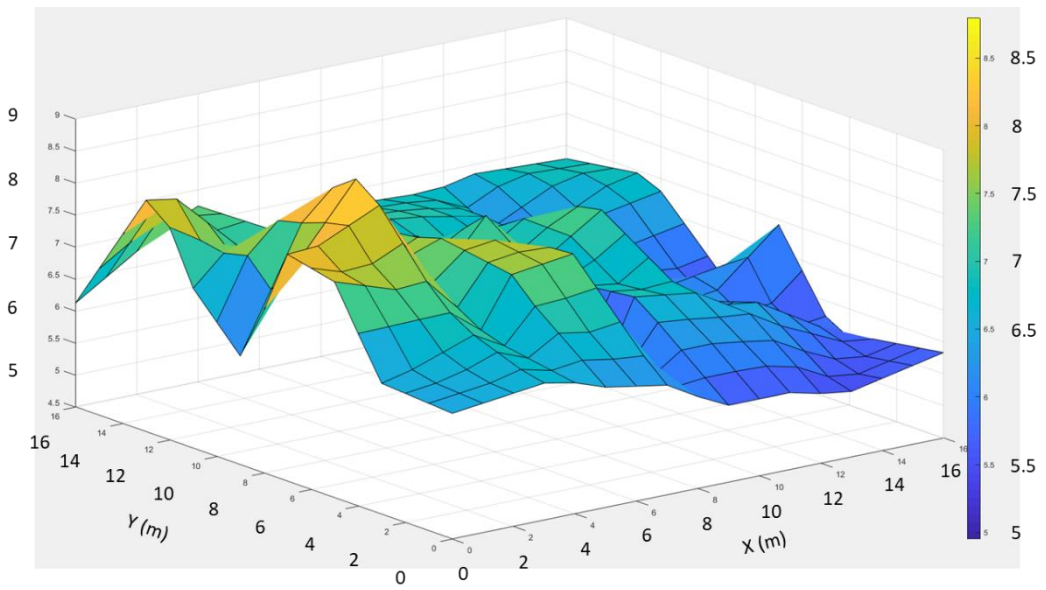


Figure 6.23: 3 m Probe Spacing Resistivity Data Plot

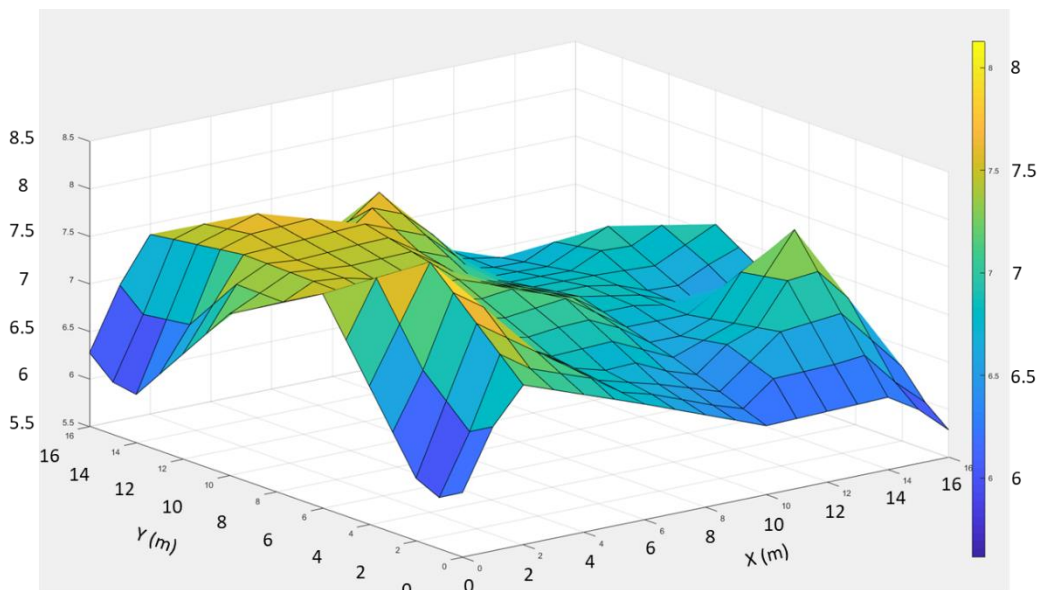


Figure 6.24: 4 m Probe Spacing Resistivity Data Plot

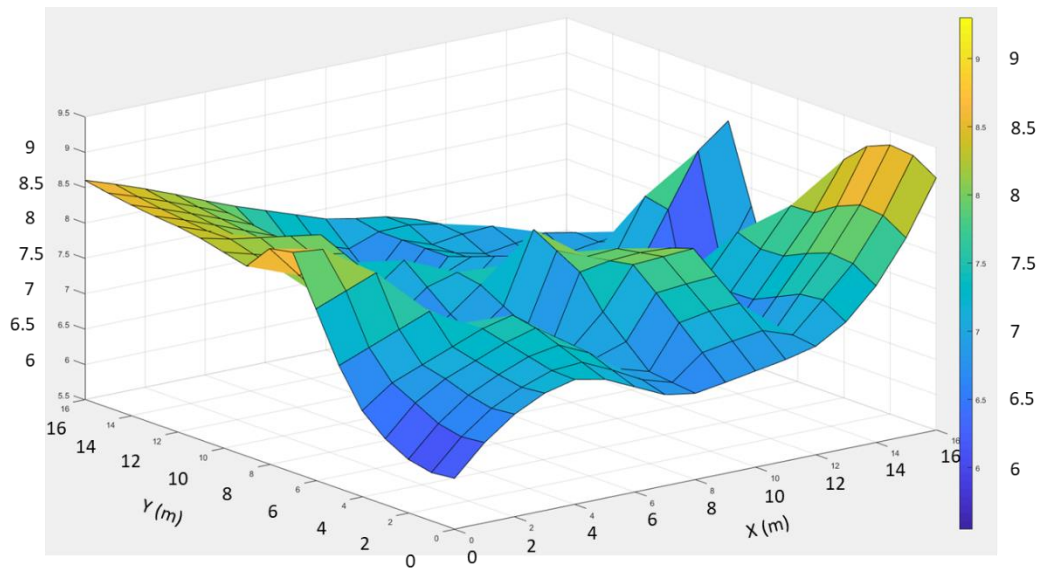


Figure 6.25: 5 m Probe Spacing Resistivity Data Plot

All the separate probe spacing data were plotted in one graph to find the apparent resistivity values in all coordinates.

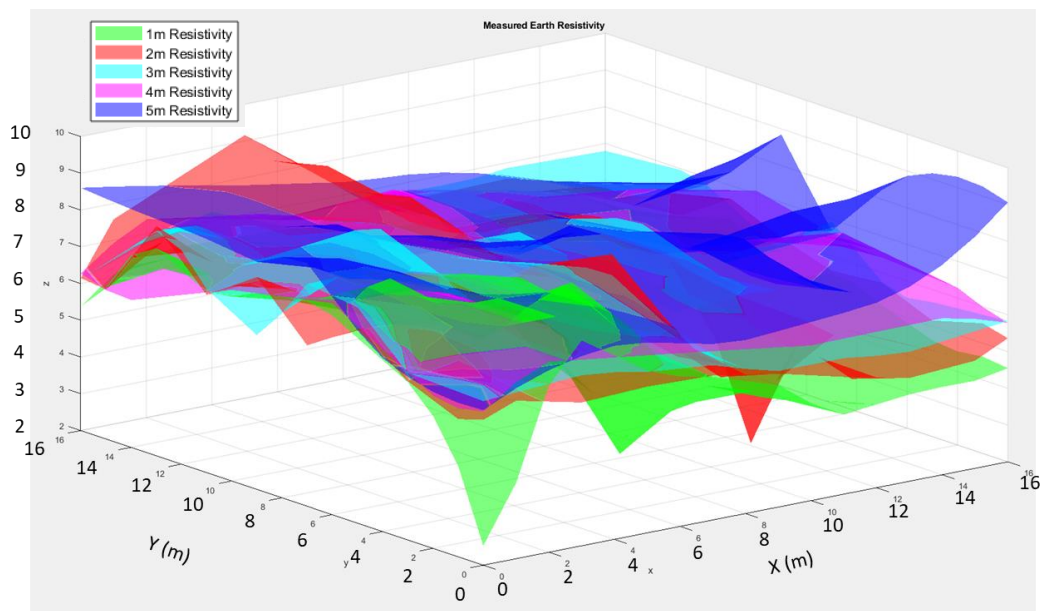


Figure 6.26: All Probe Spacing Resistivity Readings Data Plot – Location 2

From the interpolated and extrapolated resistivity data plot (Figure 6.26) the following apparent resistivity data were extracted for specific coordinates of Location 1 (20 MW Wind Power Plant in Kilinochchi).

Table 6.3: Apparent Resistivity Readings from the Data Plot

X	Y	1m	2m	3m	4m	5m
0	0	2.52652	5.95561	6.46375	6.18075	6.22019
0	4	6.66500	6.79500	7.19500	6.95750	6.71976
0	8	7.46500	7.08000	7.04500	7.47750	8.55500
0	12	7.28500	7.54500	7.82500	6.60500	8.41113
0	16	5.37694	6.14830	6.12250	6.27678	8.60402
4	0	7.00000	5.94000	6.54500	6.94750	7.26695
4	4	7.18000	7.36000	6.85500	7.22000	7.52847
4	8	7.36500	7.26000	7.46000	7.33250	7.37500
4	12	6.93000	7.24000	7.20000	7.54750	7.76264
4	16	6.44250	8.76250	7.24500	7.04000	7.96310
8	0	5.60500	5.78000	5.93500	6.47000	6.72000
8	4	3.28000	5.93000	5.83500	6.90000	7.41500
8	8	6.10000	6.83500	7.33000	7.11250	7.63000
8	12	6.30000	6.94000	6.90000	7.32750	6.73250
8	16	6.14375	7.15750	6.79875	6.74000	7.35375
12	0	4.26500	5.00000	5.58500	6.24250	7.03429
12	4	5.15500	3.98000	6.46500	6.82750	6.62583
12	8	5.42000	6.19500	4.95000	6.78000	6.58000
12	12	6.02000	6.70500	6.21500	6.73750	6.84015
12	16	5.81750	6.55000	6.75250	6.42923	6.90013
16	0	4.54923	5.36308	5.83125	5.78619	9.06350
16	4	4.87000	5.44500	5.54500	6.37000	8.86427
16	8	5.22000	5.81500	6.35000	6.77500	7.75000
16	12	5.88000	6.19000	6.80500	6.61000	6.77750
16	16	5.38192	5.80478	6.79750	5.61339	5.54820

The apparent resistivity data with probe spacing shown in Table 6.3 is used as the input data for the analysis. Genetic Algorithm is used for the optimization.

Table 6.4: Final Results Generated with Genetic Algorithm Optimization

X	Y	P1	h1	P2	h2	P3	h3	P4	h4	P5	h5	P6
0	0	1.01	4.18	3.49	2.14	0.98	7.98	1.01	5.96	0.99	4.96	4889.19
0	4	1.00	2.20	7.73	1.00	1.00	1.32	4.90	3.28	2.70	6.97	560.26
0	8	1.13	3.03	9.15	1.03	2.90	1.00	5.39	1.22	2.40	2.83	8101.64
0	12	1.10	1.61	2.33	1.00	0.97	1.45	5.80	1.47	8.01	2.01	9963.67
0	16	1.12	1.28	4.29	0.95	2.47	1.75	6.94	5.00	8.70	9.24	9160.78
4	0	1.00	2.33	5.01	1.06	1.05	1.00	8.00	6.32	9.60	6.81	9301.05
4	4	1.00	3.04	5.80	1.55	3.01	1.01	1.00	6.94	8.40	1.07	74.35
4	8	1.00	1.89	4.70	1.00	1.00	1.07	2.25	2.91	3.99	4.89	7115.75
4	12	1.00	1.93	4.60	1.00	1.07	1.00	1.00	1.00	3.50	2.14	2168.17
4	16	1.76	1.66	7.60	1.00	0.93	2.89	9.20	8.73	9.50	3.44	8312.64
8	0	1.15	3.30	7.60	1.00	2.70	1.00	7.20	5.38	5.05	1.30	7842.37
8	4	1.00	3.39	9.20	1.23	4.00	8.13	6.40	2.61	2.90	3.77	688.38
8	8	1.05	1.94	3.53	1.00	1.00	1.05	8.10	3.67	3.10	3.35	9750.15
8	12	1.03	2.05	3.40	1.00	3.20	1.00	1.00	1.70	8.39	2.22	798.37
8	16	2.13	3.43	2.03	1.00	0.90	1.77	9.60	1.36	7.60	3.01	9902.11
12	0	1.01	3.18	8.90	1.00	3.40	3.54	3.00	2.25	3.13	5.79	2910.72
12	4	1.10	1.04	0.96	1.00	4.40	1.00	1.40	1.32	9.20	1.00	1.48
12	8	2.04	5.91	9.30	1.00	3.90	1.00	1.23	1.26	6.30	8.42	50.01
12	12	1.00	3.62	4.20	1.64	7.70	1.00	8.10	1.00	2.33	6.24	2279.21
12	16	1.74	2.90	1.30	1.00	142.91	1.00	1.49	3.38	4.90	1.13	9728.86
16	0	1.17	2.24	1.04	1.00	4.57	1.45	7.17	1.98	4.90	2.65	8901.31
16	4	1.04	1.94	1.07	1.00	9.59	4.76	6.20	3.19	9.40	6.70	5343.70
16	8	1.01	1.98	1.99	1.00	1.15	1.01	1.66	2.42	9.99	8.47	9998.82
16	12	1.18	2.87	3.10	1.03	3.80	1.00	1.00	1.00	2.15	1.90	9941.12
16	16	1.05	1.01	1.78	1.26	1.71	1.41	0.93	1.16	1.97	1.14	2511.22

Each layer thickness (h) and the average resistivity of that layer ( $\rho$ ) were optimized for the minimum error using Genetic Algorithm (GA). The number of layers were limited to six to reduce the process time. The last layer  $\rho_6$  is having an infinity layer height. Table 6.4 shows the processed data using GA. This data is used to plot the three-dimensional model of the measured soil area. Here all the layer resistivities are having very low values.

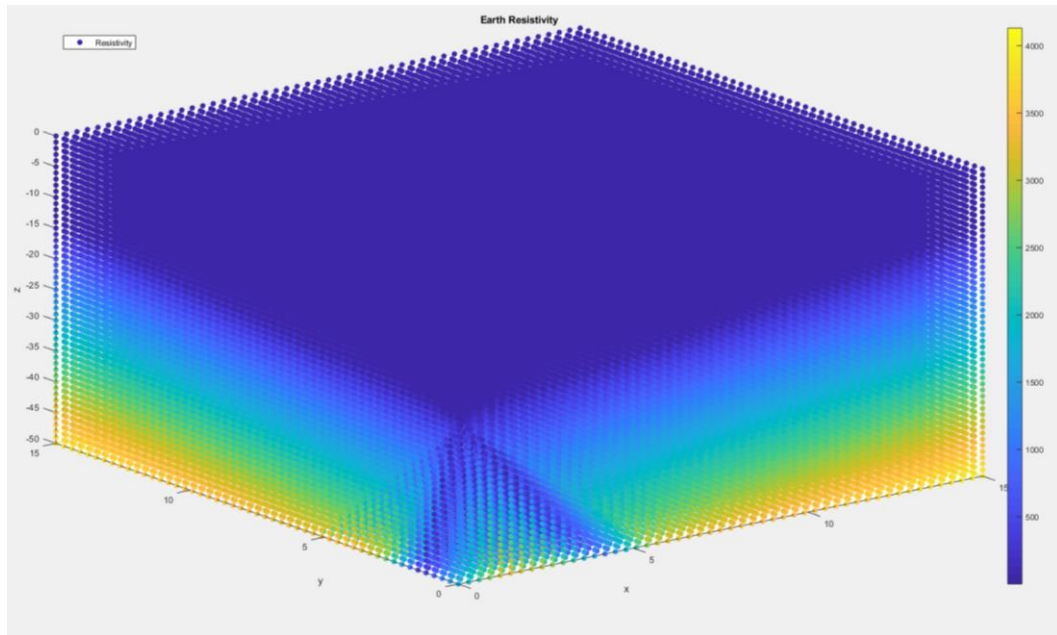


Figure 6.27: Final Results- 3 D Modelling of Earth Resistivity for Location 2

### 6.3.1. Results Validation

The 3 D model shows a resistivity variation starts from 14 m depth in one side 11 m in other side. All the resistivity readings are showing a uniform variation from top to bottom. The soil test reports are available for this location and it shows that there is a limestone rock layer starts from 9 m depth. Other than that, all the soil layers are having a uniformity from top to bottom. The soil test reports are available for this location for 6 km along the coastal zone. All the reports are showing a uniformity in soil layers and the bedrock level varies from 9 m to 12 m depth. There is a high conductivity in the soil because of the sea water penetration into the soil. Topsoil also showing a very low resistivity. Soil Test Report is attached in Appendix A.

### 7. CONCLUSIONS AND RECOMMENDATIONS

#### 7.1. Achievement of Objective and Research Outcome

“Three-dimensional modelling the earth resistivity with the help of apparent earth resistivity readings” is the objective of this research. In previous chapters propose the methodologies to achieve the objectives. The research was conducted using the proposed methodology and the data was analyzed and the result was validated.

The following can be summarized as the research outcomes:

1. The following soil model were identified
  - a. Soil with huge resistivity variation
  - b. Soil with smooth variation in resistivity
2. This model was developed using Sunde Equation and analyzed using MATLAB with Genetic Algorithm. Apparent resistivity readings were taken using Wenner four probe method.
3. Apparent soil resistivity varies with the spacing between probes. This variation can be used to identify the soil layers under the earth.
4. Field excavation and soil test reports were proved the mathematical model and the final results.

#### 7.2. Limitations of the study

The following can be listed as limitations of this research

1. The earth resistivity measurements were taken for the probe spacing of 1m, 2m, 3m, 4m and 5m only. This is because of the earth resistivity meter used for this research consists only those options. Because of this limitation in this study, the accuracy of this result become low. Using the earth resistivity meter, which can measure more in detail probe spacing values can give more accurate results.

2. The earth resistivity meter reads the average resistivity of the earth between the probe spacing. The accuracy of each unit area earth resistivity decreases with increasing probe spacing. Because it gives the average earth resistivity values. Future studies have to consider this issue and find a solution to avoid this.
3. The soil layers with huge variations in the soil resistivity is modeled and validated in this research. It is better to simulate and test the results with any soil filling or known soil models up to 15m depth in a large area with many varieties of soil and boulders in different pattern can help to test the accuracy of this model.

### **7.3. Applications and Recommendations**

This study is deriving the three-dimensional soil resistivity model using the apparent resistivity readings measured on the topsoil. This enables the users to identify the soil layer pattern in a required geographical area.

This helps to identify an optimum grounding system for an electrical installation, lightning protection system et cetera at the design stage to increase the safety and reliability with a cost optimization.

This can be used to design the foundation and other excavation works at the construction stage

Level of corrosion can be estimated for the underground items like piling, pipeline laying with this earth resistivity profiles.




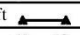

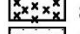
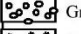
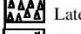




## 8. References

- [1] IEEE Guide for Measuring Earth Resistivity, Ground Impedance, and Earth Surface Potentials of a Grounding System, IEEE, 2012.
- [2] BS 7430:2011 Code of practice for protective earthing of electrical installations, 2011.
- [3] Ioannis F. Gonos and Ioannis A. Stathopoulos, "Estimation of Multilayer Soil Parameters Using Genetic Algorithms," *IEEE TRANSACTIONS ON POWER DELIVERY*, vol. 20, no. 1, pp. 100-106, 2005.
- [4] Lee Weng Choun, Mohd Zainal Abidin Ab Kadir, Chandima Gomes and Wan Fatinhamamah Wan Ahmad, "Analysis of Earth Resistance of Electrodes and Soil Resistivity at Different Environments," in *International Conference on Lightning Protection (ICLP)*, Vienna, Austria, 2012.
- [5] T. Islam, Z. Chik, M. M. Mustafa and H. Sanusi, "Estimation of Soil Electrical Properties in a Multilayer Earth Model with Boundary Element Formulation," *Mathematical Problems in Engineering*, vol. 2012, p. 13, 2012.
- [6] Mohamed Nayel, Boyang Lu, Yu Tian and Yingzhen Zhao, "Study of Soil Resistivity Measurements in Vertical Two-Layer Soil Model," Department of Electric and Electronic Engineering, Xi'an Jiaotong-Liverpool University, Suzhou, China.
- [7] Xiaobin Cao, Guangning Wu, Shenglin Li, Weiming Zhou and RuiFang.Li, "A Simple formula of Grounding Grid Resistance in Vertical Two-Layer Soil," in *IEEE/PES Transmission and Distribution Conference and Exposition*, Chicago, IL, USA, 2008.
- [8] Predrag D. Rancid, Zoran P. Stajic and Bojana S. ToSid, "Analysis of Linear Ground Electrodes Placed invertical Three-Layer Earth," *IEEE TRANSACTIONS ON MAGNETICS*, vol. 32, no. 3, pp. 1505-1508, 1996.
- [9] Maria Clementina Caputo and Lorenzo De Carlo, *Field Measurement of Hydraulic Conductivity of Rocks*, Bari, Italy: Intech, 2011, pp. 285-306.
- [10] Fernando Visconti and José Miguel de Paz, *Electrical Conductivity Measurements in Agriculture: The Assessment of Soil Salinity*, València, Spain: New Trends and Developments in Metrology, 2016.



- [11] Zeyad Abu Heen and Shehda Muhsen, "Application of Vertical Electrical Sounding for Delineation of Sea Water Intrusion into the Freshwater Aquifer of Southern Governorates of Gaza Strip, Palestine," *IUG Journal of Natural Studies, Islamic University, Gaza*, vol. 24, no. 2, pp. 07-20, 2016.
- [12] Adekitan Israel Aderibigbe, Isaac Samuel, Bukola Adetokun and Shomefun Tobi, "Monte Carlo Simulation Approach to Soil Layer Resistivity Modelling for Grounding System Design," *International Journal of Applied Engineering Research*, vol. 12, no. 23, pp. 13759-13766, 2017.
- [13] W. C. J. and D. L. A. X. Lu, "The electric fields and currents produced by induction logging instruments in anisotropic media," *Geophysics*, vol. 67, no. 2, p. 478-483, 2002.
- [14] H. A. Abdel-Ghany, A. M. Azmy, N. I. Elkalashy and E. M. Rashad, "Optimizing DG Penetration in Distribution Networks Concerning Protection Schemes and Technical Impact," *Electric Power System Research*, vol. 128, pp. 113-122, 2015.
- [15] "Soil - Resistivity," The Engineering ToolBox, 2013. [Online]. Available: [https://www.engineeringtoolbox.com/soil-resistivity-d\\_1865.html](https://www.engineeringtoolbox.com/soil-resistivity-d_1865.html). [Accessed 5 12 2019].



		<b>ENGINEERING &amp; LABORATORY SERVICES (PVT) LTD.</b> <b>SITE INVESTIGATIONS DIVISION</b>			NO 62/3, Neelammahara Road, Katuwawala, Sri Lanka. Tel: 0114 309 494		Format No: ELS-SI-02																							
<b>Project</b>		<b>Additional Soil investigation for the proposed Wind Power Project at Elephant Pass</b>				<b>Borehole No</b>		<b>BH-01(P1)</b>																						
<b>Client</b>		<b>M/s.Beta Power (Pvt) Ltd.</b>				<b>Sheet</b>		<b>2 of 2</b>																						
<b>Location</b>		Elephant Pass		Rig	Edico	Core Diameter		54mm																						
<b>Date of Started</b>		04.03.2014		Drilling Method		Rotary		Casing depth		9.60m																				
<b>Date of Finished</b>		05.03.2014		Casing Diameter		76mm		Elevation (MSL)		Coordinates																				
Depth (m)	Sa. Cond	Sa.No.	Sa.Type	Reduced level	Depth (m)	Legend	Soil Description	Field Records (SPT)				Moisture Content - %																		
								15cm	15cm	15cm	N	Undrained Shear Strength - t/m																		
10.00							Ground level																							
11.00			CS				Offwhite,brown LIMESTONE	Cr=73%	RQD=00%																					
12.00			CS		11.10		Offwhite,brown LIMESTONE	Cr=93%	RQD=00%																					
13.00					12.60		The borehole was terminated at a depth of 13.60m																							
14.00																														
15.00																														
16.00																														
17.00																														
18.00																														
19.00																														
20.00																														
Sample Key / Test Key												Remarks		Logged By:																
SPT Where full 0.3m penetration has not been achieved the number of blows for the quoted penetration is given (not N-value)			D - Disturbed Sample			SS -SPT Sample			W - Water Sample			WS-Wash Sample			UD- Undisturbed Sample			CS- Core Sample			Cr - Core Recovery (%)			RQD-Rock Quality Designation (%)			Existing ground level considered as the zero level		Nishantha	
GWL -Ground Water Level observed inside the Borehole, after the saturation			N - Natural Moisture Content			L - Atterberg Limit Test			G - Grain Size Analysis			SG -Specific Gravity Test			B - Bulk Density			V - Vane Shear Test			C - Consolidation			Supervised By:						
NE -Not Encountered			CU - Consolidated Undrained			UU-Unconsolidated Undrained			pH - Chemical			O - Organic content			SO <sub>4</sub> <sup>2-</sup> - Sulphate Content			Cl - Chloride Content			Lakshitha									
HB -Hammer Bounce			Completely Weathered Rock			Fresh Rock														Drilled By:										
FD -Free Down			Highly Weathered Rock																	Sumathipala										
 Made Ground		 Silt		 Gravel		 Laterite Nodules		 Silty Sand																						
 Clay		 Sand		 Organic Matter																										

## Appendix B – Research papers